

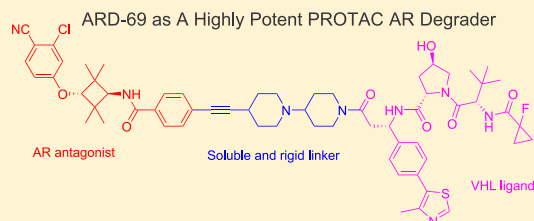
Discovery of ARD-69 as a Highly Potent Proteolysis Targeting Chimera (PROTAC) Degradator of Androgen Receptor (AR) for the Treatment of Prostate Cancer

Xin Han,^{†,‡,∇} Chao Wang,^{†,‡,∇,▲} Chong Qin,^{†,‡,∇} Weiguo Xiang,^{†,‡,∇} Ester Fernandez-Salas,^{†,||} Chao-Yie Yang,^{†,‡} Mi Wang,^{†,‡} Lijie Zhao,^{†,‡} Tianfeng Xu,^{†,‡} Krishnapriya Chinnaswamy,[#] James Delprosto,[#] Jeanne Stuckey,[#] and Shaomeng Wang^{*,†,‡,§,⊥,lib}

[†]The Rogel Cancer Center, [‡]Departments of Internal Medicine, [§]Pharmacology, ^{||}Pathology, [⊥]Medicinal Chemistry, and [#]Life Sciences Institute, University of Michigan, Ann Arbor, Michigan 48109, United States

Supporting Information

ABSTRACT: We report herein the discovery of highly potent PROTAC degraders of androgen receptor (AR), as exemplified by compound 34 (ARD-69). ARD-69 induces degradation of AR protein in AR-positive prostate cancer cell lines in a dose- and time-dependent manner. ARD-69 achieves DC₅₀ values of 0.86, 0.76, and 10.4 nM in LNCaP, VCaP, and 22Rv1 AR+ prostate cancer cell lines, respectively. ARD-69 is capable of reducing the AR protein level by >95% in these prostate cancer cell lines and effectively suppressing AR-regulated gene expression. ARD-69 potently inhibits cell growth in these AR-positive prostate cancer cell lines and is >100 times more potent than AR antagonists. A single dose of ARD-69 effectively reduces the level of AR protein in xenograft tumor tissue in mice. Further optimization of ARD-69 may ultimately lead to a new therapy for AR+, castration-resistant prostate cancer.



- Achieving <1 nM DC₅₀ value in LNCaP and VCaP AR+ prostate cancer cell lines
- Effectively reducing the mRNA level of PSA, FKBP5 and TMPRSS2 at concentrations as low as <10 nM
- Inhibiting cell growth with IC₅₀ values of <1 nM in LNCaP and VCaP cell lines.
- A single dose effectively reducing AR and PSA in VCaP xenograft tumor tissue in mice

INTRODUCTION

Despite improvements in medical treatments over the past three decades, prostate cancer (PCa) remains a significant cause of cancer-related death, and is second only to lung cancer among men in developed countries.^{1,2} In addition to surgery and radiotherapy, androgen deprivation therapies (ADTs) are frontline treatments for prostate cancer patients with high-risk localized disease, and second-generation antiandrogens, such as abiraterone and enzalutamide, have been shown to benefit patients with advanced prostate cancer.^{3,4} Nevertheless, patients who progress to metastatic castration-resistant prostate cancer (mCRPC), a hormone-refractory form of the disease, face a high mortality rate and no cure is currently available.^{5,6}

The androgen receptor (AR) and its downstream signaling play a critical role in the development and progression of both localized and metastatic prostate cancer.⁷ Previous strategies that successfully target AR signaling have focused on blocking androgen synthesis by drugs such as abiraterone and inhibition of AR function by AR antagonists such as enzalutamide and apalutamide (ARN-509).^{8–14} However, such agents become ineffective in advanced prostate cancer with AR gene amplification, mutation, and alternate splicing.^{15,16} It is very clear, however, that in most patients with CRPC, the AR protein continues to be expressed and tumors are still dependent on AR signaling. Consequently, AR is an attractive therapeutic target for mCRPC.^{17,18}

In the last few years, the proteolysis targeting chimera (PROTAC) strategy has gained momentum with its promise in the discovery and development of completely new types of small-molecule therapeutics by inducing targeted protein degradation.^{19–25} A PROTAC molecule is a heterobifunctional small molecule containing one ligand, which binds to the target protein of interest, and a second ligand for an E3 ligase system, tethered together by a chemical linker.²⁶ Because AR protein plays a key role in CRPC, AR degraders designed based upon the PROTAC concept could be potentially very effective for the treatment of CRPC when the disease becomes resistant to AR antagonists or to androgen synthesis inhibitors.^{27–30} Naito et al. have recently reported AR degraders designed based on the PROTAC concept, which were named specific and nongenetic inhibitors of apoptosis protein (IAP)-dependent protein erasers (SNIPERS).³¹ An AR SNIPER molecule, e.g., compound 1 was designed using an AR antagonist and a ligand for the cellular inhibitor of apoptosis protein 1 (cIAP1) as the E3 ligase. While SNIPER AR degraders are effective in inducing partial degradation of the AR protein in cells, they induce the autoubiquitylation and proteasomal degradation of the cIAP1 protein, the E3 ligase needed for induced degradation of AR protein, thus limiting their AR degradation efficiency and

Received: October 21, 2018

Published: January 10, 2019

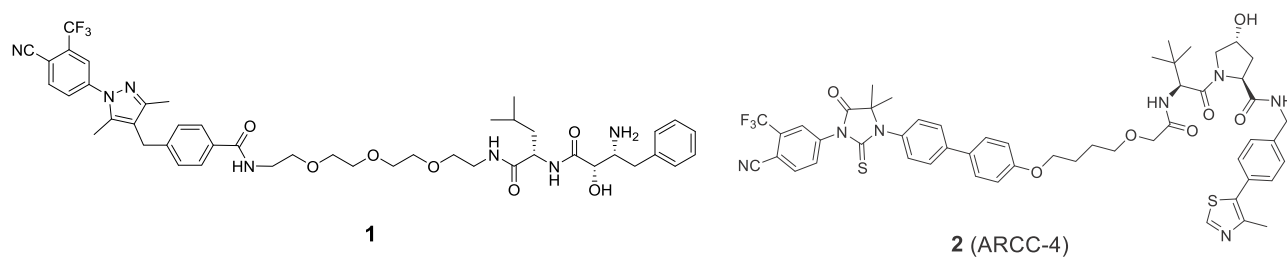


Figure 1. Chemical structures of two previously reported AR degraders.

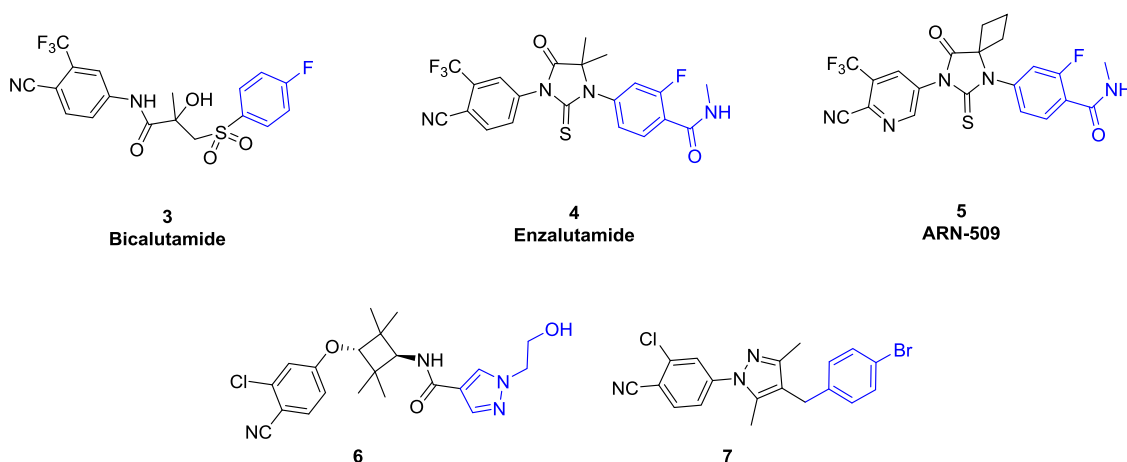


Figure 2. Chemical structures of representative AR antagonists.

therapeutic efficacy. Compound 2 (ARCC-4) has been recently reported as another PROTAC degrader, which was designed using enzalutamide as the AR antagonist and a von Hippel-Lindau (VHL) ligand.^{27,32} ARCC-4 was shown to be more potent and effective than enzalutamide at inducing apoptosis and inhibiting proliferation of AR-amplified prostate cancer cells (Figure 1).^{27,32}

In the present study, we report our design, synthesis, and evaluation of PROTAC AR degraders prepared using several different classes of AR antagonists (Figure 2). Because the cereblon/cullin 4A and VHL/cullin 2 neddylation degradation systems have been successfully employed for the design of PROTAC degraders for different proteins, we have evaluated both these types of E3 ligases for the design of AR PROTAC degraders. The linker in a PROTAC molecule plays a key role for its degradation potency and efficacy and accordingly, we have performed extensive optimization of the linker. This study has resulted in the discovery of highly potent PROTAC AR degraders (hereafter called AR degraders), exemplified by compound 34 (ARD-69). This compound (ARD-69) achieves $DC_{50} < 1$ nM and $D_{max} > 95\%$ in LNCaP and VCaP AR+ prostate cancer cell lines. Our present study lays the foundation for the development of a completely new class of therapeutic agents for the treatment of CRPC.

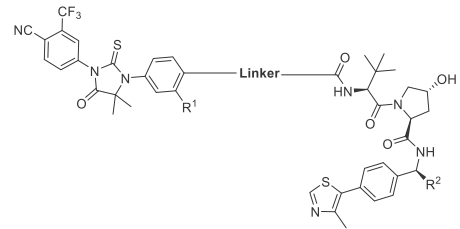
RESULTS AND DISCUSSION

In the design of PROTAC AR degraders, it is critical to identify a suitable site for tethering in both an AR antagonist and an E3 ligase ligand. Although co-crystal structures of AR agonists complexed with AR and co-crystal structures of AR antagonists bound to mutated AR proteins in an agonist conformation are available,³³ no crystal structure of AR in an antagonist conformation complexed with an AR antagonist is available.

However, the aryl group in different AR antagonists (shown in blue in Figure 2) has been extensively modified and a large number of substituents on this aryl group have been shown to be well tolerated. The extensive available structure–activity relationship (SAR) data suggest that this aryl group is exposed to solvent, making it a potentially suitable site for tethering in the design of PROTAC AR degraders. Indeed, in both compounds 1 and 2, this aryl group was employed as the tethering site. Therefore, we have employed the corresponding aryl group in different AR antagonists for our design and synthesis of PROTAC AR degraders.

We designed and synthesized a series of potential PROTAC AR degraders (8–25) using as enzalutamide (4), a Food and Drug Administration-approved AR antagonist, and a potent, previously reported VHL ligand,³⁴ and different linkers to tether the AR antagonist and VHL ligand together (Table 1). We first evaluated these compounds in the AR-positive (AR+) LNCaP cells for their ability to induce degradation of AR protein at different concentrations by Western blotting and obtained the data summarized in Table 1.

Our Western blotting data showed that compounds 8–11, which contain a linker with two to five methylene groups, effectively reduce AR protein level at 0.1, 1, and 10 μ M concentrations. However, the maximum reduction of AR protein achieved by compounds 8–11 at 0.1–10 μ M is only ~30%. Compound 12 containing a linker with six methylene groups effectively reduces the AR protein by 54% at 0.1 μ M and by 84% at 1 μ M and is therefore a more potent AR degrader. Interestingly, at 10 μ M, compound 12 reduces AR protein by 64%, less than that at 1 μ M, probably due to the “hook” effect that has been observed previously for PROTAC molecules.²¹ Accordingly, we evaluated several highly potent AR degraders at a concentration range of 1–100 nM to better determine their potency. Our data showed that compound 13, containing a

Table 1. Optimization of Linker Length, Composition, and VHL Moiety^a


Compound	Linker	R ¹	R ²	% AR protein degradation in LNCaP cells (μM)			
				0.01	0.1	1	10
DMSO	--			0	0	0	0
4	--			--	--	30	19
8		F	H	--	26	35	28
9		F	H	--	15	23	33
10		F	H	--	16	20	25
11		F	H	--	11	25	29
12		F	H	--	54	84	64
13		F	H	8	29	65	--
14		F	H	15	66	87	--
15		F	H	10	48	88	--
16		F	H	11	48	86	--
17		F	H	--	30	69	75
18		F	H	--	32	35	40
19		H	H	30	63	96	--
20		H	H	--	50	80	80
21		H	Me	37	61	92	--
22		H	Me	28	48	89	--
23		H	Me	34	51	78	--
24		H	Me	--	3	31	28
25		H	Me	--	0	12	0

^aAll of the data were average of three independent experiments with a treatment time of 6 h.

linker with 7 methylene groups appears to be less potent than **12**, but compounds **14–16**, containing a linker with 8–10 methylene groups, have potencies similar to **12**. Compound **17**, containing a linker with 11 methylene groups, is less potent

than compounds **15** and **16**. These data indicate that in these PROTAC AR degraders, there is an optimal linker length of 11–12 atoms for achieving the most effective AR degradation.

We next investigated the chemical composition of the linker, by keeping the total linker length approximately the same as that in compound **15** or **16**. Compound **18** with a poly(ethylene glycol) linker fails to induce AR degradation at 0.1, 1, and 10 μM, indicating that both the linker length and the linker chemical composition are important for a PROTAC AR degrader to effectively induce AR degradation.

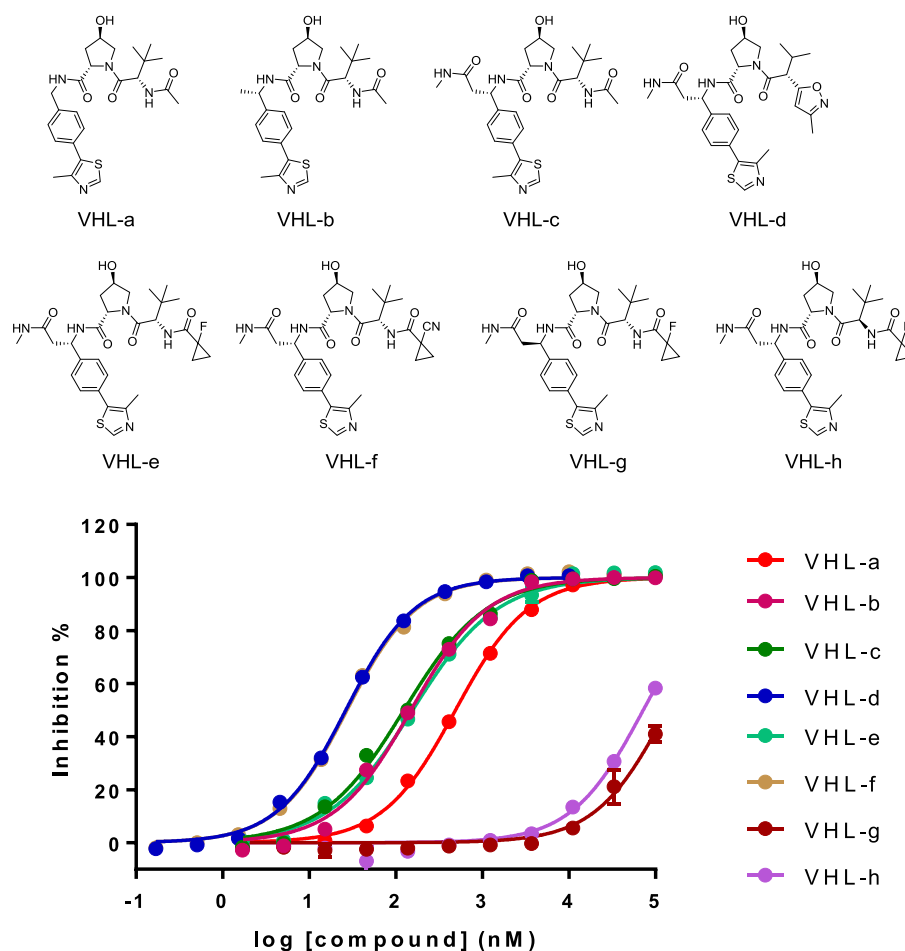
Compounds **8–18** contain an amide group tethering the phenyl group in enzalutamide with the linker. We replaced the amide bond in the linker with an ethynyl group, which we had used successfully in our design of extremely potent bromodomain and extra-terminal (BET) degraders.²³ To increase the solubility of the compounds, we introduced a pyridine group into the linker, directly connected to the ethynyl group. This led to the design and synthesis of compound **19**, which effectively reduces AR protein level by 30, 63, and 96% at 10 nM, 100 nM, and 1 μM, respectively, and is therefore a very potent and effective AR degrader. To further improve its solubility, we incorporated a piperazinyl group into the linker in compound **19**, yielding compound **20**. Compound **20** effectively reduces AR protein level by 50, 80, and 80% at 100 nM, 1 μM, and 10 μM, respectively.

In the design of VHL ligands, it has been shown that introduction of an (*S*)-methyl group (*R*²) significantly improves the binding affinity to VHL.¹⁹ To confirm this, we developed a fluorescence polarization (FP)-based binding assay for VHL protein (Supporting Information) and tested the binding affinities of two VHL ligands, VHL-a and VHL-b. Our binding data showed that VHL-a and VHL-b bind to VHL protein with IC₅₀ values of 458 and 164 nM (Figure 3). Hence, VHL-b is 3 times more potent than VHL-a. Accordingly, we introduced an (*S*)-methyl group (*R*²) into compound **20**, yielding compound **21**. Compound **21** effectively reduces AR protein by 37, 61, and 92% at 10 nM, 100 nM, and 1 μM, respectively, and is more potent than **20**.

Encouraged by the high potency of compound **21** in induction of AR degradation, we further explored the linker length in **21** by synthesis of compounds **22–25**, which have either a shorter or longer linker. Compound **22** with one more methylene group and compound **23** with one less methylene group than the linker in compound **21** achieve very similar potencies compared to **21**. However, compound **24** with two less methylene groups than compound **21** induces AR degradation by 3, 31, and 28% at 100 nM, 1 μM, and 10 μM, respectively, and is thus much less potent and effective than **21**. Compound **25** with three less methylene groups than compound **21** is completely ineffective in inducing AR degradation at 0.1–10 μM. Taken together, our data demonstrate that both the length and composition of the linker in a PROTAC AR degrader play a major role in induction of AR degradation.

In our design of PROTAC AR degraders (**8–25**), we tethered enzalutamide (**4**) to the terminal amide group in the VHL ligand. We also investigated other possible tethering positions in the VHL ligand for the design of AR degraders.

Based upon a number of co-crystal structures of VHL ligands in complex with VHL protein (e.g., PDB: 4W9H and 5LLI),^{33–36} the (*S*)-methyl group in VHL-b is exposed to the solvent environment and can be used as a possible tethering point for the design of AR degraders. To facilitate the synthesis



VHL	VHL-a	VHL-b	VHL-c	VHL-d	VHL-e	VHL-f	VHL-g	VHL-h
IC ₅₀ ± SD (nM)	458 ± 33	164 ± 13	130 ± 5	26.8 ± 1.1	190 ± 36	28.6 ± 1.1	179 ± 37 (μM)	78 ± 6 (μM)

Figure 3. Chemical structures of VHL ligands and their binding affinities to VHL protein as determined in our FP-based binding assay (Supporting Information).

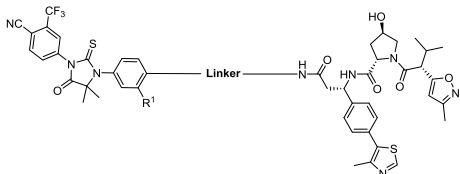
of new AR degraders, we appended an amide group to the (*S*)-methyl group and synthesized three VHL ligands (Figure 3) with different “tail” groups based upon previous published SAR studies on VHL ligands.^{34,35} These three ligands, VHL-c, VHL-d and VHL-e all bind to VHL with a high affinity, and VHL-d is the most potent with an IC₅₀ value of 26.8 nM to VHL (Figure 3). We next designed and synthesized two potential AR degraders (26 and 27) using enzalutamide, VHL-d and the linkers used in the two potent AR degraders 15 and 21. Western blotting analysis showed that both 26 and 27 effectively induce AR degradation in a dose-dependent manner with >50% of AR protein being reduced at 0.1 μM and >80% at 1 μM in the LNCaP cell line.

On the basis of the promising AR degradation data for 27, we synthesized compound 28 with a shorter and more rigid linker than in 27. Compared to compound 27, compound 28 is similarly potent and effective in reducing the AR protein level in the LNCaP cell line, at 0.01–1 μM.

We next designed and synthesized compound 29 also with a rigid linker, but its length is similar to that in compound 28.

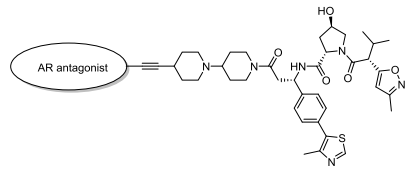
Compound 29 induces 81% of AR degradation at 100 nM and 97% at 1 μM in the LNCaP cell line and is therefore a potent and effective AR degrader (Table 2).

Next, we designed and synthesized a number of potential AR degraders using compound 29 as the template AR degrader and other four AR antagonists shown in Figure 2. The results are summarized in Table 3. Compound 30 was synthesized by replacing the enzalutamide “core” structure with that of ARN-509 (apalutamide). Compound 30 effectively induces AR degradation in the LNCaP cell line and has a potency similar to that of compound 29. Compound 31 was synthesized by replacing the enzalutamide core structure with that of bicalutamide. Compound 31 is much less potent than compounds 29 and 30 in reducing AR protein level in the LNCaP cell line. Compound 32 was synthesized by replacing the enzalutamide core structure in 29 with a potent AR antagonist reported by Guo et al. from Pfizer.¹⁰ Compound 32 reduces AR protein by 76, 98, and 99% at 10 nM, 100 nM, and 1 μM, respectively, in the LNCaP cell line. In direct comparison, compound 32 is more potent than compounds 29 and 30.

Table 2. Investigation of the Middle Linking Site from the VHL ligand^a


Compound	Linker	R ¹	% AR protein degradation in LNCaP cells (μM)			
			0.01	0.1	1	10
DMSO	--		0	0	0	0
4	--		--	--	30	19
26		F	11	50	87	--
27		H	27	75	94	--
28		H	22	72	93	--
29		H	20	81	97	--

^aAll of the data were average of three independent experiments with a treatment time of 6 h.

Table 3. Investigation of the Effect of Different AR Antagonists^a


Compound	AR antagonist	/ AR protein degradation in LNCaP cells (μM)			
		0.01	0.1	1	10
DMSO	--	0	0	0	0
29		20	81	97	--
30		38	80	95	--
31		--	18	34	35
32		76	98	99	--
33		--	65	93	78

^aAll of the data were average of three independent experiments with a treatment time of 6 h.

Compound 33 was synthesized by replacing the enzalutamide core structure in 29 with an AR antagonist reported by the

Takeda Corporation.¹⁴ Compound 33 reduces AR protein by 65, 93, and 78% at 100 nM, 1 μM, and 10 μM, respectively, in the LNCaP cell line. Our data thus showed that compound 32 containing the AR antagonist reported by Guo et al. from Pfizer¹⁰ is the most potent AR degrader from this series of AR degraders designed using the same linker and the same VHL ligand but different AR antagonists.

Because the VHL ligand plays a key role in our designed PROTAC AR degraders induction of AR degradation, we synthesized two new VHL ligands (VHL-e and VHL-f) on the basis of a recent study.³⁵ Our binding data showed that both VHL-e and VHL-f bind to VHL protein with a high affinity with IC₅₀ values of 190 and 28.6 nM, respectively. To investigate the stereospecificity of these compounds, we also synthesized VHL-g and VHL-h by changing a chiral center in VHL-e. VHL-g and VHL-h bind to VHL protein with IC₅₀ values of 179 and 78 μM, respectively, and are >100 times less potent than VHL-e, highlighting the importance of stereochemistry for both chiral centers in the binding to VHL protein.

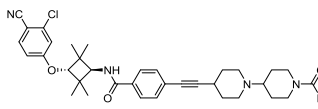
Employing VHL-e and VHL-f as the VHL ligands and using compound 32 as the template AR degrader molecule, we synthesized compounds 34 and 35 (Table 4). For the purpose of comparison, we also synthesized compound 36 by employing VHL-c as the VHL ligand and compound 32 as the template molecule.

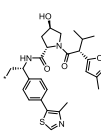
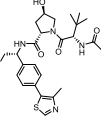
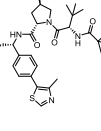
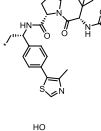
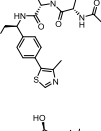
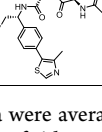
Western blotting showed that compounds 34 and 35 are highly potent and effective in reducing AR protein in the LNCaP cell line and both compounds reduce the AR protein level by >75% at 10 nM and >95% at both 100 nM and 1 μM concentrations. Compound 36 is also very effective and reduces the AR protein level by 39, 77, and 99% at 10 nM, 100 nM, and 1 μM, respectively. Hence, compounds 34 and 35 represent two extremely potent AR degraders.

We synthesized two control degrader compounds (37 and 38) by employing VHL-g and VHL-h as the VHL ligands and compound 34 as the template degrader molecule. Our Western blotting showed that both 37 and 38 fail to reduce AR protein level at 0.1–10 μM in the LNCaP cell line (Table 4). This suggests that strong binding of our designed PROTAC AR degraders to VHL protein is necessary for effective induction of AR degradation.

Cereblon ligands have been used successfully in the design of highly potent degraders of BET protein^{20,23} and other proteins.^{37–39} We sought to determine if cereblon ligands can be used for the design of effective AR degraders. We synthesized compounds 40 and 41 using two cereblon ligands and the same linkers as those in two potent AR degraders 32 and 39 designed using a VHL ligand. Although 32 and 39 effectively induce AR degradation at 10 nM, 100 nM, and 1 μM concentrations in the LNCaP cell line, compounds 40 and 41 have only a modest effect in reducing the level of AR protein. Taken together, these data show that VHL ligands are very suitable for the design of highly potent AR degraders, but more studies are needed to determine if the cereblon/cullin 4A E3 ligase system can be used for the design of highly potent and effective AR degraders (Table 5).

We further evaluated three potent AR degraders, compounds 32, 34, and 35, for their dose-dependent AR degradation in the LNCaP cell line, with compound 6 included as the AR antagonist control. Our Western blotting data showed that each of these three AR degraders induces AR degradation in a dose-dependent manner, whereas the AR antagonist (6) is completely ineffective, even at 10 μM. While compounds 32, 34,

Table 4. Investigation of VHL Ligands^a


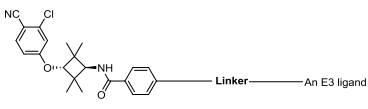
Compound	R	% AR protein degradation in LNCaP cells (μM)			
		0.01	0.1	1	10
DMSO	--	0	0	0	0
6	--	--	--	24	47
32		76	98	99	--
34		89	99	100	--
35		76	99	100	--
36		39	77	99	--
37		--	<5	<5	<5
38		--	<5	<5	<5

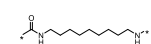
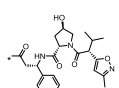
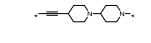
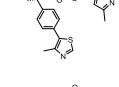
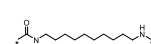
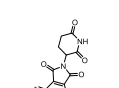
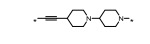
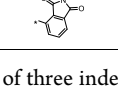
^aAll of the data were average of three independent experiments with a treatment time of 6 h.

and 35 induce partial AR degradation at 10 nM, they all induce essentially complete AR degradation at both 100 nM and 1 μM. Based on the data obtained at 10 nM, compound 34 appears to be the most potent AR degrader among 32, 34, and 35, and consequently, we pursued an extensive investigation of compound 34 (ARD-69).

We evaluated the kinetics of ARD-69 in induction of AR degradation at 100 nM in the LNCaP and VCaP AR+ cell lines. Our data showed that ARD-69 effectively reduces the AR protein level within 2 h and achieves near-complete AR depletion with a 4 h treatment (Figure 4). Our kinetic data thus showed that induced AR degradation by ARD-69 in LNCaP and VCaP cells is rapid.

We further evaluated ARD-69 in LNCaP, VCaP, and 22Rv1 cell lines for its potency in inducing AR degradation with a 24 h treatment time and obtained the data summarized in Figure 5. ARD-69 achieves DC₅₀ (the drug concentration that results in

Table 5. Investigation of Different E3 Ligands^a


Compound	Linker	E3 Ligands	% of AR protein degradation in LNCaP cells (μM)			
			0.01	0.1	1	10
DMSO	--	--	0	0	0	0
39			43	91	96	--
32			76	98	99	--
40			--	7	20	5
41			--	2	25	20

^aAll of the data were average of three independent experiments with a treatment time of 6 h.

50% protein degradation) values of 0.86 and 0.76 nM in the LNCaP and VCaP cell lines, respectively, and >95% AR degradation at 10 nM in both cell lines. ARD-69 achieves a DC₅₀ of 10.4 nM and near-complete degradation at 1 μM in 22Rv1 cells.

We next investigated the ability of ARD-69 to suppress AR-regulated gene expression in LNCaP and VCaP cell lines, with a potent AR antagonist (6) included as the control (Figures 6 and 7). Our data showed that ARD-69 effectively suppresses the expression of *PSA*, *TMPRSS2*, and *FKBP5* genes in both LNCaP and VCaP cell lines in a dose-dependent manner and is capable of reducing the mRNA level of both *PSA* and *TMPRSS2* genes by >50% at 10 nM. In addition, ARD-69 is also very effective in suppressing the *ERG* gene in VCaP cell lines in a dose-dependent manner. In direct comparison, the AR degrader ARD-69 is >100 times more potent than the potent AR antagonist 6 in suppressing the AR-regulated gene transcription in both LNCaP and VCaP cell lines.

Because AR signaling drives cell growth for AR-positive prostate cancer cells, we tested the ability of ARD-69 to inhibit cell growth, with enzalutamide (4) and compound 6 included as the AR antagonist controls. Our data showed that ARD-69 is highly potent in inhibition of cell growth in both LNCaP and VCaP cell lines and achieves IC₅₀ values of 0.25 and 0.34 nM in the LNCaP and VCaP cell lines, respectively (Figure 8). In the 22Rv1 cell line, compound 34 (ARD-69) achieves an IC₅₀ value of 183 nM and AR antagonists 4 and 6 have IC₅₀ values of >10 μM. Therefore, ARD-69 is >100 times more potent than enzalutamide (4) and compound 6 in LNCaP, VCaP, and 22Rv1 AR+ prostate cancer cell lines.

We investigated the mechanism of AR degradation induced by ARD-69 in LNCaP and VCaP cells. Our data showed that AR degradation induced by ARD-69 can be effectively blocked by pretreatment with an AR antagonist (6), a VHL ligand (VHL-d), a NEDD8 activating E1 enzyme inhibitor (MLN4924), or a proteasome inhibitor (MG132) in both LNCaP (Figure 9) and VCaP (Figure 10) cell lines. These mechanistic data clearly demonstrate that ARD-69 is a bona fide PROTAC AR degrader.

We examined the pharmacodynamics (PD) of ARD-69 in the VCaP xenograft tumor tissue in mice (Figure 11). Our PD data showed that a single administration of ARD-69 at 50 mg/kg via

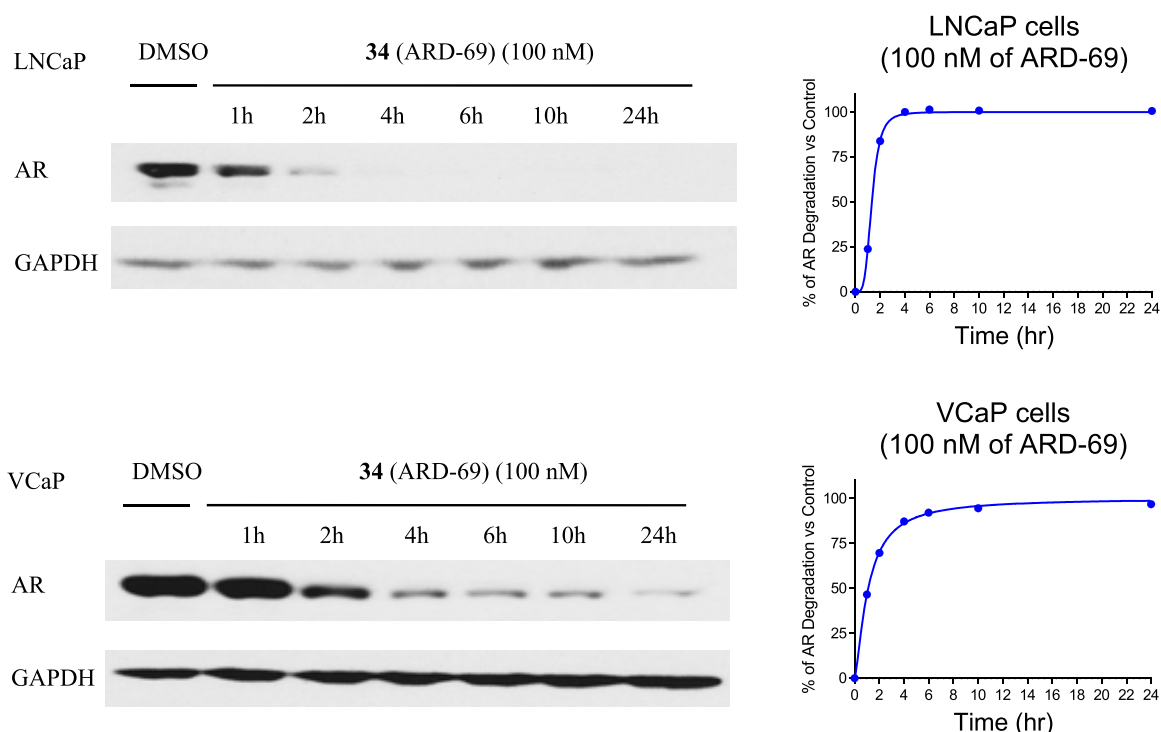


Figure 4. Western blotting analysis of AR protein in LNCaP cells treated with AR degrader **34** (ARD-69), with glyceraldehyde 3-phosphate dehydrogenase (GAPDH) used as the loading control. Cells were treated with 100 nM of ARD-69 for indicated time points.

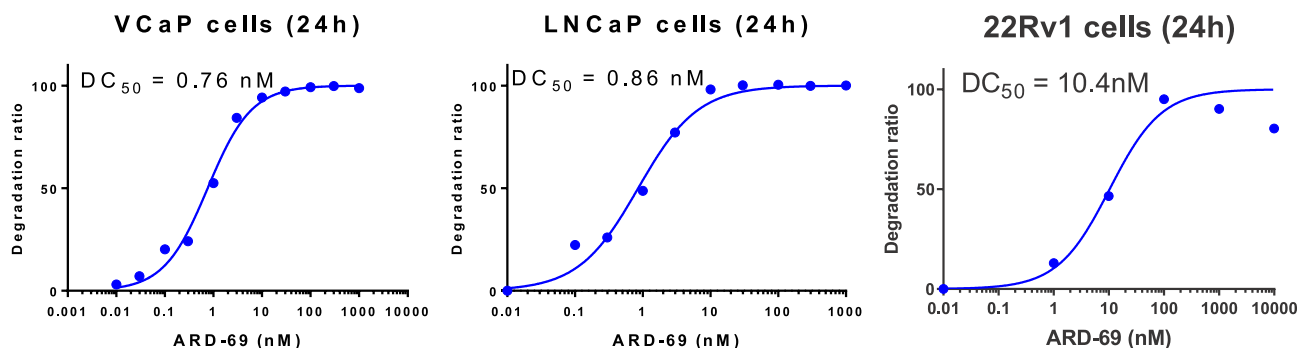


Figure 5. Examination of dose-dependent AR degradation by **34** (ARD-69) in LNCaP, VCaP, and 22Rv1 prostate cancer cell lines. Cells were treated for 24 h.

intraperitoneal (IP) injection effectively reduces the level of AR protein, starting at 3 h and with the effect persisting for at least 48 h. Consistent with the profound decrease of the AR protein, the level of PSA protein is also effectively reduced at the 3 h time point with the effect persisting for 24–48 h.

CHEMISTRY

The synthesis of VHL ligands (**49a**, **49b**) is outlined in [Scheme 1](#). Briefly, (4-bromophenyl)methanamine (**42a**) was protected by Boc_2O to generate **43a**. An intermediate (**44**) was obtained through the Heck reaction of **43a** and 4-methylthiazole, and subsequent deprotection of the Boc group gave compound **45a**. Amide coupling of **46** with **47** followed by hydrolysis of the methyl ester produced the key intermediate (**48**). Amidation of **48** with **45a** in the presence of 1-[bis(dimethylamino)methylene]-1*H*-1,2,3-triazolo[4,5-*b*]-pyridinium 3-oxide hexafluorophosphate (HATU) and *N,N*-diisopropylethylamine (DIPEA) at room temperature (rt) in dimethylformamide (DMF) gave the target compound (**49a**).

As shown in [Scheme 2](#), compounds **8–17** were synthesized by the amidation of intermediate **52** and the VHL ligand (**49a**). Intermediate **52** was produced by amidation of compound **50** and a series of amines. Compound **50** was synthesized by the hydrolysis of commercial enzalutamide (**4**). Compound **18** was synthesized from the amidation reaction of compound **53**, which was prepared from intermediate **50**. The synthesis of compound **26** was through several amidation reactions starting from intermediate **50**.

The synthesis of compound **19** is shown in [Scheme 3](#). First, the key intermediate (**57**) was synthesized by coupling of compounds **55** and **56**. Then, the Sonogashira coupling reaction of **57** with 1-bromo-4-ethynylbenzene in the presence of cuprous iodide (CuI) and $\text{PdCl}_2(\text{PPh}_3)_2$ at 100 °C in DMF/triethylamine (TEA) gave compound **58**. The intermediate (**59**) was obtained from **58** in the presence of 2-hydroxy-2-methylpropanenitrile. The target compound (**19**) can be obtained through the amidation reaction of VHL ligand (**49a**) with **60**, which in turn was derived from intermediate **59**.

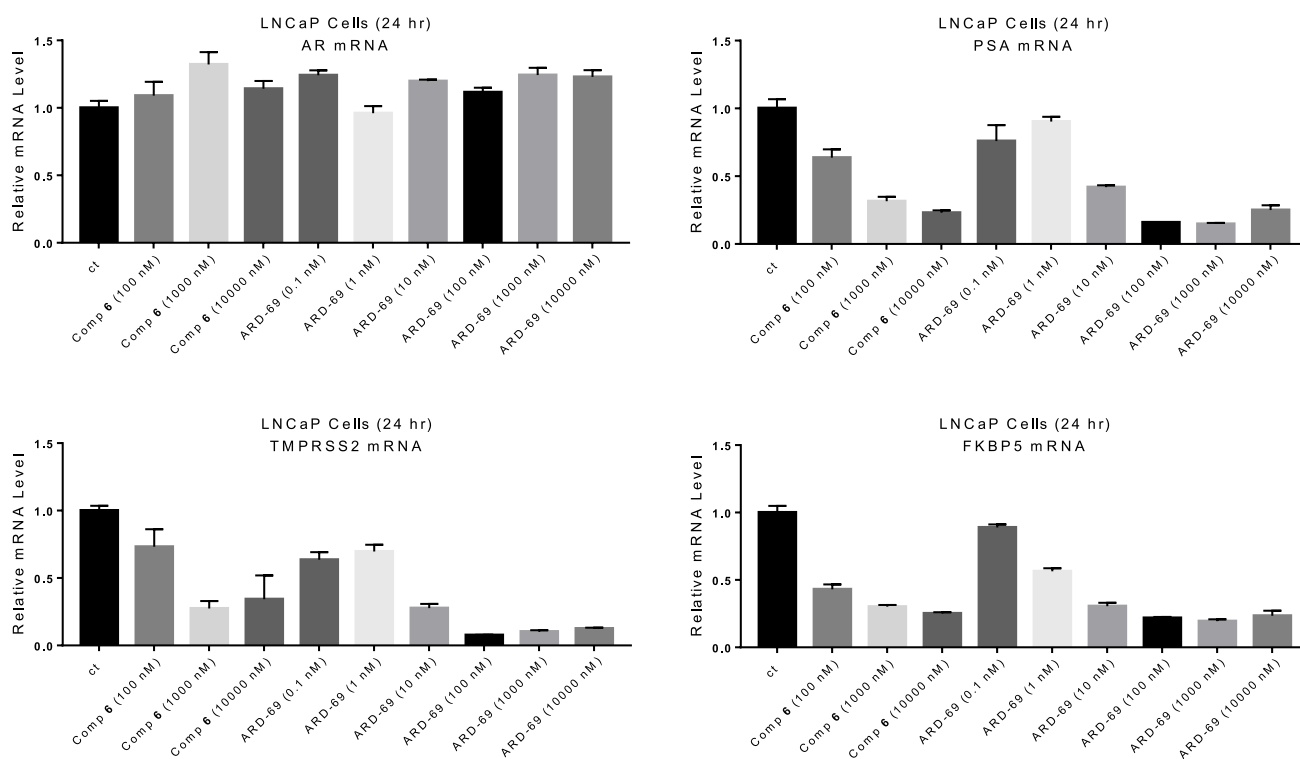


Figure 6. Suppression of AR-regulated gene expression in the LNCaP cell line by the AR degrader 34 (ARD-69) and the AR antagonist 6. LNCaP cells were treated for 24 h and quantitative real-time polymerase chain reaction (qRT-PCR) was performed to determine the mRNA levels for AR and AR-regulated genes.

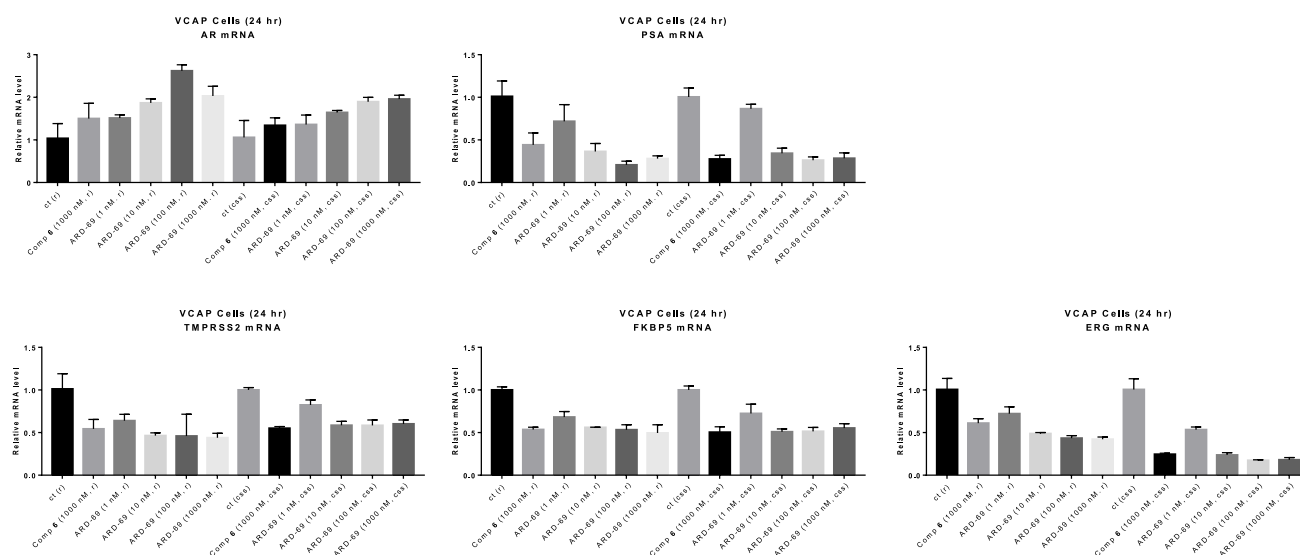


Figure 7. Suppression of AR-regulated gene expression in the VCaP cell line by AR degrader 34 (ARD-69) and AR antagonist 6. VCaP cells were treated for 24 h and qRT-PCR was performed to determine the mRNA levels for AR and AR-regulated genes. r, regular serum; css, charcoal stripped serum.

As shown in Scheme 4, compounds 20–25, 27, and 28 were synthesized according to the following procedure. A Heck reaction of compounds 61 and 62 gave the key intermediate (63). The other key intermediate (68) was made through four steps from the starting material (64) according to a published method.⁴⁰ Then, a Sonogashira coupling reaction of 69 and 70 in the presence of dichlorobisphosphonium ($\text{PdCl}_2(\text{PPh}_3)_2$), cuprous iodide (CuI) and triethylamine (TEA) in dry DMF gave the key linker portion (71). A mixture of 71 and acetone cyanohydrin was heated to 80 °C and stirred for 4 h. The

medium was concentrated and dried under vacuum to yield 72, which was used in the next step without further purification. A mixture of 4-isothiocyanato-2-(trifluoromethyl)benzotrile and 72 in DMF was stirred overnight. Then, MeOH and 2 N HCl were added to this mixture to give the cyclized intermediate (73). A substitution reaction between 73 and *tert*-butyl 2-bromoacetate in the presence of K_2CO_3 and KI gave the key intermediate (74). Amidation of 74 and the VHL ligand (49) gave the target compounds (20–25). Compounds 27 and 28 were obtained through two amidation reactions.

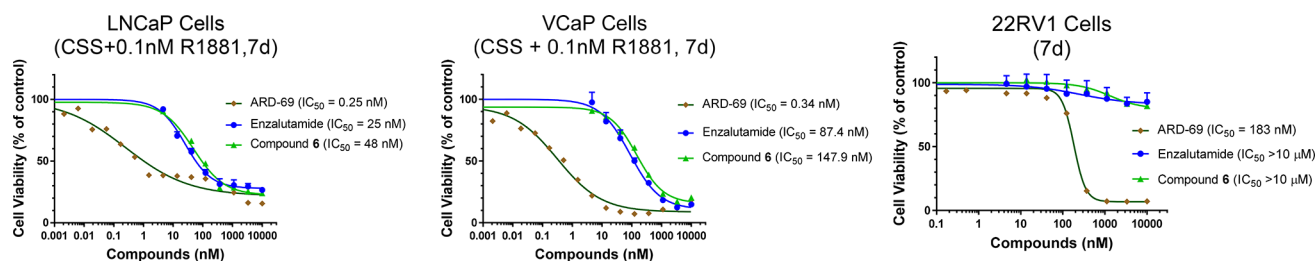


Figure 8. Cell growth inhibition in LNCaP, VCaP, and 22Rv1 cells treated with AR degrader **34** (ARD-69) and two AR antagonists enzalutamide (**4**) and **6**. LNCaP and VCaP cells were treated with different compounds in charcoal stripped medium in the presence of 0.1 nM of AR agonist R1881 for 7 days, and 22Rv1 cells were treated with a regular culture medium for 7 days. Cell viability was determined by a 2-(2-methoxy-4-nitrophenyl)-3-(4-nitrophenyl)-5-(2,4-disulphonyl)-2H-tetrazolium (WST-8) assay.

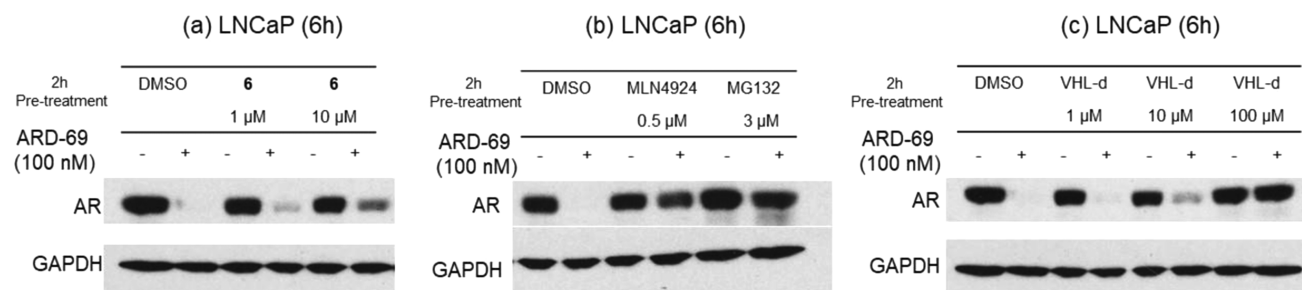


Figure 9. Mechanistic investigation of AR degradation induced by **34** (ARD-69) in LNCaP cells. Cells were pretreated with AR antagonist **6**, VHL-d, MLN4924, and MG132, followed by 6 h treatment with ARD-69 at 100 nM.

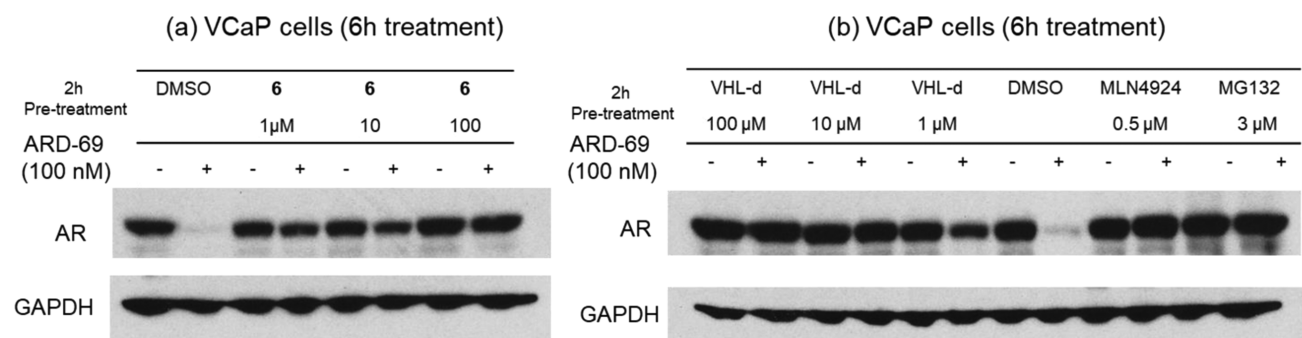


Figure 10. Mechanistic investigation of AR degradation induced by **34** (ARD-69) in VCaP cells. Cells were pretreated with AR antagonist **6**, VHL-d, MLN4924, and MG132, followed by 6 h treatment with **34** (ARD-69) at 100 nM.

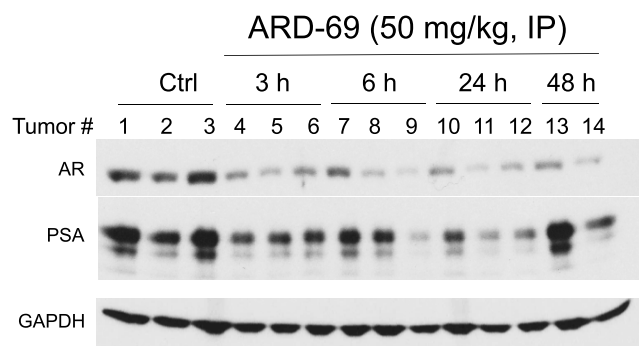
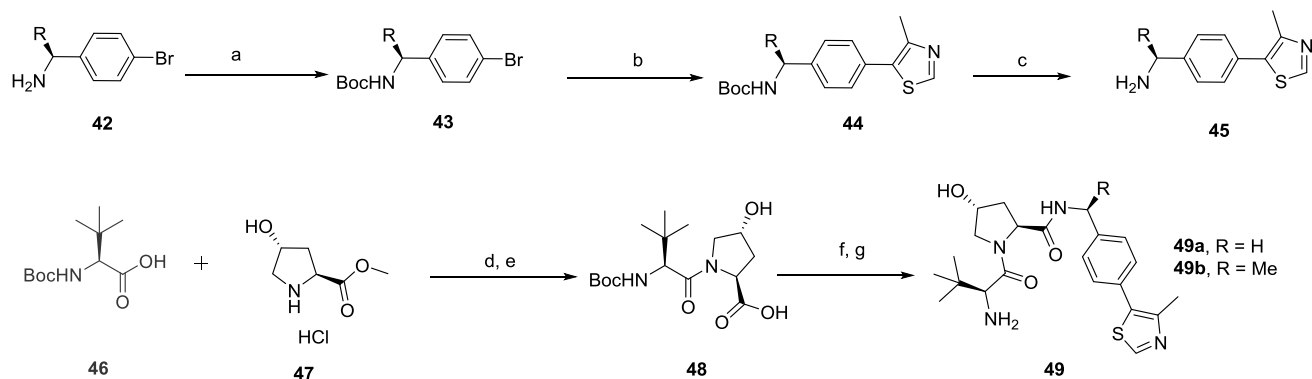


Figure 11. Pharmacodynamics (PD) study of AR degrader **34** (ARD-69) in VCaP tumor tissue in mice. Severe combined immunodeficient (SCID) mice bearing xenograft VCaP tumors were treated with a single dose of **34** (ARD-69) (IP, 50 mg/kg). Tumor tissues were harvested at the indicated time points for immunoblotting.

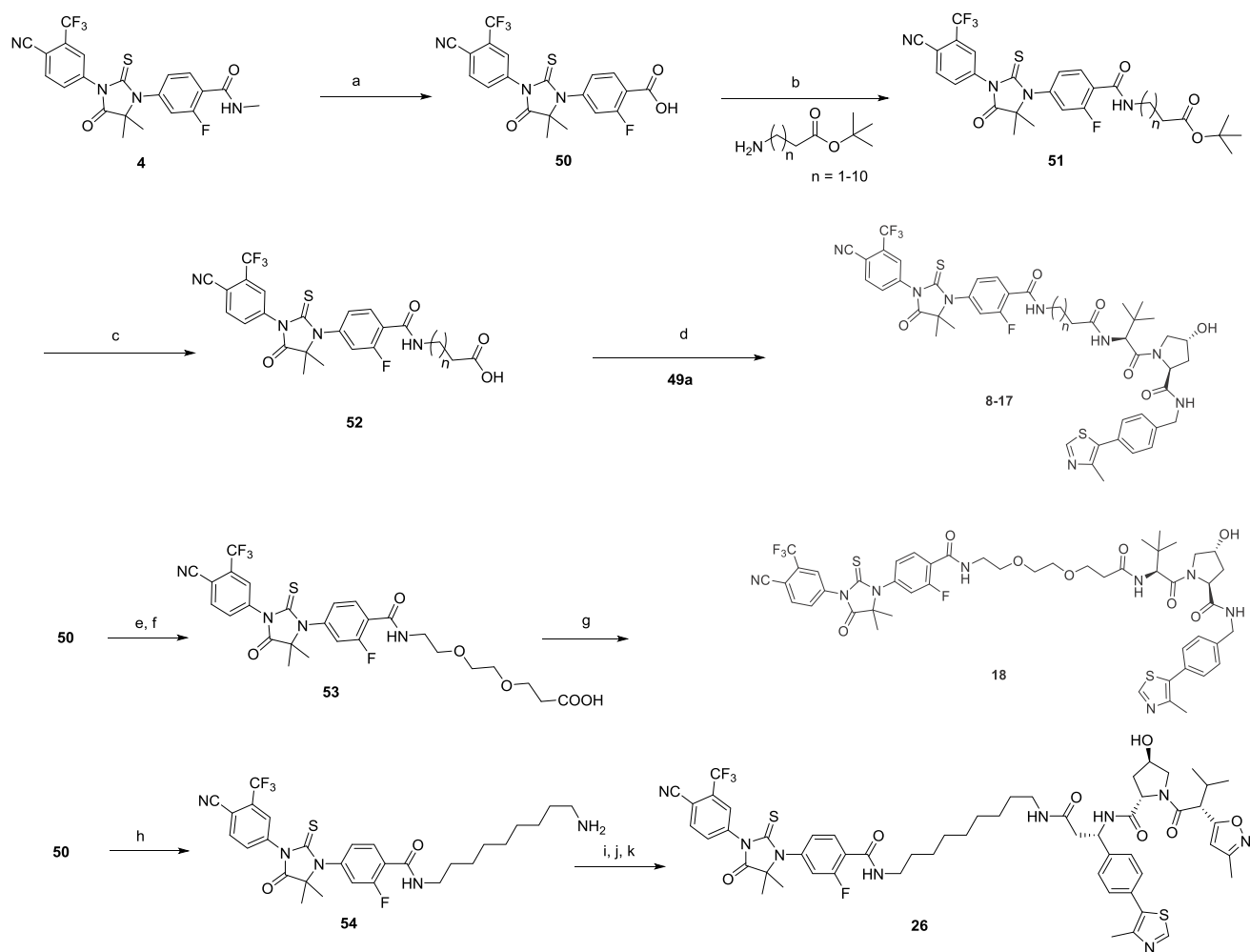
The synthesis of compounds **29** and **30** is shown in [Scheme 5](#). A Sonogashira coupling reaction of **75** and **76** in the presence of dichlorobispalladium ($\text{PdCl}_2(\text{PPh}_3)_2$), cuprous iodide (CuI),

and TEA in dry DMF gave the key linker portion (**77**). A mixture of **77** and acetone cyanohydrin was heated to 80 °C and stirred for 4 h. The medium was concentrated and dried under vacuum to give **78**, which was used in the next step without further purification. A mixture of 4-isothiocyanato-2-(trifluoromethyl)benzotrile and **78** in DMF was stirred overnight at rt. Then, MeOH and 2 N HCl were added to this mixture to give the cyclized intermediate (**79**). A substitution reaction of **79** with *tert*-butyl 4-bromobutanoate in the presence of K_2CO_3 and KI gave the key intermediate (**80**). Amidation of **80** and **63** gave the compound **81**. In the last step, the compounds **29** and **30** were obtained through amidation reaction of the intermediate **81** with **68**.

Syntheses of compounds **32** and **34–36** are shown in [Scheme 6](#). Compound **83** was synthesized from the Sonogashira coupling reaction of the starting material (**82**) and **76**. Compound **84** was made through the substitution reaction of intermediate **83** and *tert*-butyl 4-bromopiperidine-1-carboxylate. As shown in [Scheme 6](#), the key intermediate (**88**) was synthesized in two steps. Compound **89** can be obtained from the amidation reaction of compound **88** with different amino

Scheme 1. VHL Ligands 49^a

^aReaction conditions: (a) (Boc)₂O, NaHCO₃, EtOAc/H₂O; (b) 4-methylthiazole, Pd(OAc)₂, KOAc, 90 °C; (c) trifluoroacetyl (TFA), dichloromethane (DCM), rt; (d) HATU, DIPEA, DMF, rt; (e) LiOH, tetrahydrofuran (THF), H₂O; (f) HATU, DIPEA, DMF, rt; (g) TFA, DCM, rt.

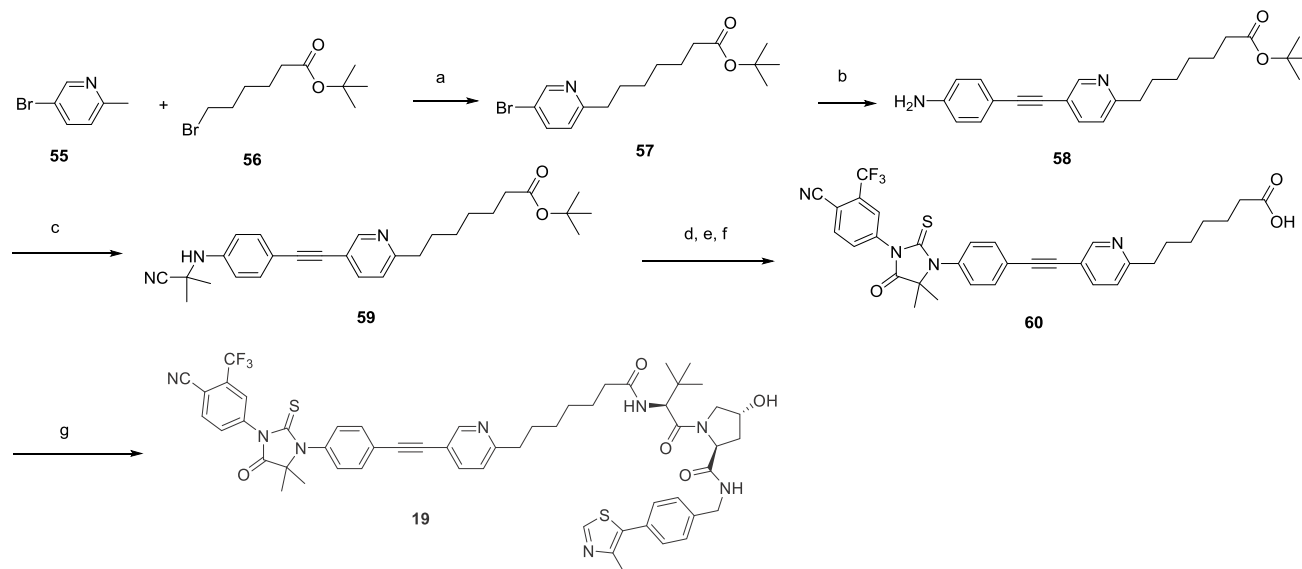
Scheme 2. Compounds 8–18 and 26^a

^aReaction conditions: (a) concd HCl, dioxane, reflux; (b) HATU, DIPEA, DMF, rt; (c) TFA, DCM, rt; (d) HATU, DIPEA, DMF, rt. (e) HATU, DIPEA, DMF, rt; (f) TFA, DCM, rt; (g) HATU, DIPEA, DMF, rt; (h) HATU, DIPEA, DMF, rt; (i) HATU, DIPEA, DMF, rt; (j) TFA, DCM, rt; (k) HATU, DIPEA, DMF, rt.

acids. Finally, the target compounds were obtained through the amidation of intermediate 89 and various VHL fragments.

Compound 31 was synthesized according to the method shown in Scheme 7. A substitution reaction of compounds 90

and 91 gave the key intermediate (92). The key AR antagonist portion (96) can be obtained from the reaction of compounds 93 and 94 followed by a further oxidation reaction. A Sonogashira coupling reaction of compounds 96 and 92 gave

Scheme 3. Compound 19^a

^aReaction conditions: (a) *n*-BuLi, THF, rt; (b) CuI, PdCl₂(PPh₃)₂, DMF/TEA, 100 °C; (c) 2-hydroxy-2-methylpropanenitrile, reflux; (d) 4-isothiocyanato-2-(trifluoromethyl)benzonitrile, DMF, 80 °C; (e) MeOH, 2 N HCl, reflux; (f) TFA, DCM, rt; (g) HATU, DIPEA, DMF, rt.

compound 97, and the target compound 31 was obtained by two amidation reactions.

The synthesis of compound 33 is shown in Scheme 8. Compound 101 was synthesized by the Michael addition reaction of compound 99 with 100, and compound 104 was made by the reaction of compound 101 with NH₂NH₂. The reaction of compound 102 with compound 85 gave the AR antagonist (103). A Sonogashira coupling reaction of 103 with 92 in the presence of CuI and PdCl₂(PPh₃)₂ at rt in DMF/TEA gave compound 104. Finally, the target compound 33 was obtained from an amidation reaction.

As shown in Scheme 9, compounds 39–41 were made according to the following procedure. In detail, compound 107 was synthesized by the amidation reaction of compounds 87 and 106. Compound 108 was made by hydrolysis reaction of intermediate 107, and intermediate 109 was synthesized by the amidation of compound 108 with nonane-1,9-diamine. Finally, the target compound (39) was synthesized by two amidation reactions. Compound 41 was made through the substitution reaction of 88 with 111, and compound 40 was synthesized by the substitution reaction of 111 and 112, which was produced by amidation reaction of decane-1,10-diamine with compound 108.

In Scheme 10, compounds 37 and 38 were synthesized according to the previously published methods as shown in Scheme 4.

CONCLUSIONS

In this study, we have designed, synthesized, and evaluated a series of PROTAC AR degraders using five different AR antagonists and ligands for VHL/cullin 2 and cereblon/cullin 4A E3 ligases. We also performed extensive optimization of the linker tethering the AR antagonist portion and the E3 ligand portion in our designed AR degraders. Our efforts have yielded highly potent and effective AR degraders, as exemplified by compound 34 (ARD-69). ARD-69 is effective in inducing AR degradation at concentrations lower than 1 nM in LNCaP and VCaP prostate cancer cell lines with a 24 h treatment time and is

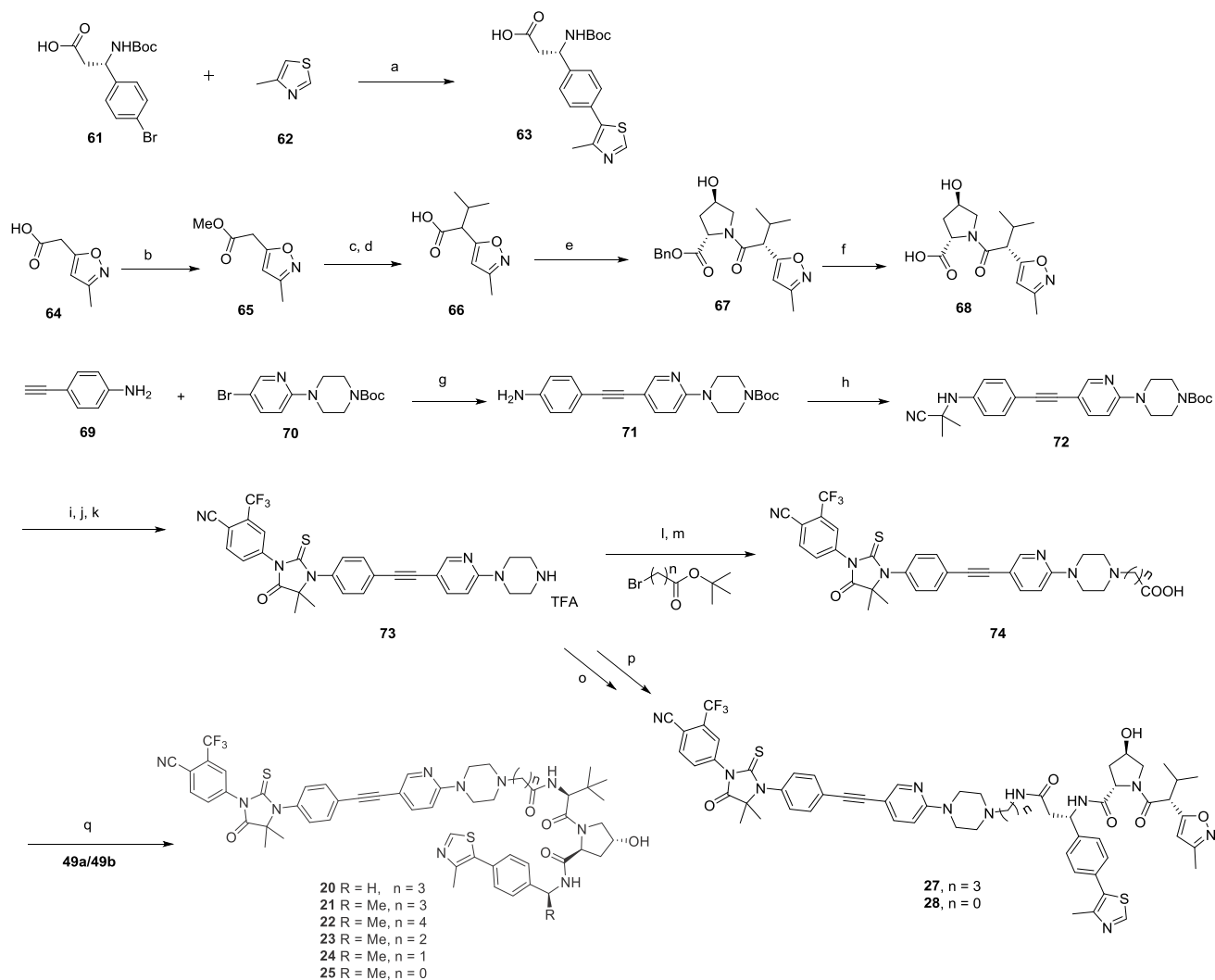
capable of achieving complete AR degradation in these cell lines. ARD-69 effectively suppresses AR-regulated gene expression in a dose-dependent manner and is effective at concentrations as low as 10 nM in the LNCaP and VCaP cell lines with 24 h treatment time. It potently inhibits cell growth in the LNCaP, VCaP, and 22Rv1 prostate cancer cell lines and is >100 times more potent than the two AR antagonists that were tested. In particular, ARD-69 achieves subnanomolar IC₅₀ values in the LNCaP and VCaP cell lines. A single dose of ARD-69 also effectively reduces AR and PSA proteins in VCaP xenograft tumor tissues in mice for more than 48 h. Taken together, our data demonstrate that ARD-69 is an extremely potent AR degrader and that further optimization of ARD-69 may yield a new class of drugs for the treatment of mCRPC.

EXPERIMENTAL SECTION

Chemistry. *General Experiment and Information.* Unless otherwise noted, all purchased reagents were used as received without further purification. ¹H NMR and ¹³C NMR spectra were recorded on a Bruker Avance 400 MHz spectrometer. ¹H NMR spectra were reported in parts per million (ppm) downfield from tetramethylsilane. All ¹³C NMR spectra were reported in ppm and obtained with ¹H decoupling. In reported spectral data, the format (δ) chemical shift (multiplicity, *J* values in Hz, integration) was used with the following abbreviations: s = singlet, d = doublet, t = triplet, q = quartet, m = multiplet. Mass spectral (MS) analysis was carried out with a Waters ultraperformance liquid chromatography (UPLC) mass spectrometer. The final compounds were all purified by C18 reverse-phase preparative high-performance liquid chromatography (HPLC) column with solvent A (0.1% TFA in H₂O) and solvent B (0.1% TFA in CH₃CN) as eluents. The purity of all of the final compounds was confirmed to be >95% by UPLC–MS or UPLC.

General Procedure for Synthesis of Compounds 8–17. Conc HCl (5 mL) was added to a solution of enzalutamide (4) (4.64 g, 10 mmol) in dioxane (50 mL). The reaction mixture was refluxed for 2 h. The reaction mixture was quenched with H₂O and extracted with DCM. The organic layer was separated, washed with brine, dried, and evaporated. The final compound 50 was obtained by flash column chromatography (hexane/EtOAc = 4:1) in 95% yield.

DIPEA (5 equiv) and HATU (1.2 equiv) were added to a solution of compound 50 (451 mg, 1 mmol) and a series of linear amines (1.1

Scheme 4. Compounds 20–25, 27, and 28^a

^aReaction conditions: (a) Pd(OAc)₂, KOAc, 90 °C; (b) MeOH, H₂SO₄, 70 °C; (c) 2-iodopropane, *t*-BuOK, THF, rt; MeOH, (d) LiOH, MeOH/H₂O, rt; (e) benzyl (2*S*,4*R*)-4-hydroxypyrrolidine-2-carboxylate hydrochloride, HATU, DIPEA, DMF, rt; (f) Pd–C, H₂, MeOH, rt; (g) CuI, PdCl₂(PPh₃)₂, DMF/TEA, 100 °C; (h) 2-hydroxy-2-methylpropanenitrile, reflux; (i) 4-isothiocyanato-2-(trifluoromethyl)benzonitrile, DMF, 80 °C; (j) MeOH, 2 N HCl, reflux; (k) TFA, DCM, rt; (l) K₂CO₃, KI, CH₃CN, reflux; (m) TFA, DCM, rt; (o) HATU, DIPEA, DMF, rt; (p) TFA, DCM, rt; (q) HATU, DIPEA, DMF, rt.

equiv) in DMF (2 mL). After 30 min at rt, the mixture was subject to HPLC purification to afford compound **51** in 80–90% yields.

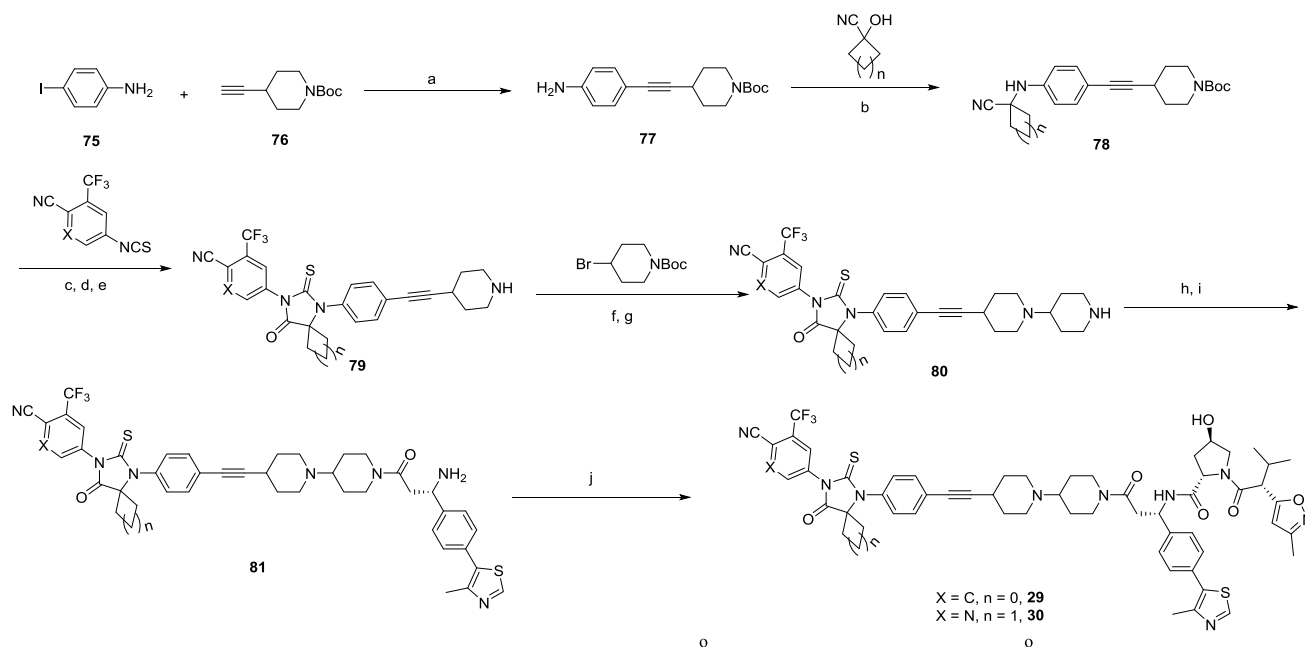
A solution of compound **51** in 1:1 TFA/DCM was stirred at rt for 30 min. The solvents were evaporated under reduced pressure to give the corresponding deprotected intermediate **52** (TFA salt) that was used in the following reactions without further purification (95% yield).

DIPEA (5 equiv) and HATU (1.2 equiv) were added to a solution of compound **52** (52.2 mg, 0.1 mmol) and compound **49a** (1.1 equiv) in DMF (2 mL). After 30 min at rt, the mixture was subject to HPLC purification to afford compound **8** in 90% yield. Following the procedures used to prepare compound **8**, compounds **9–17** with different chain lengths were obtained by the same methods.

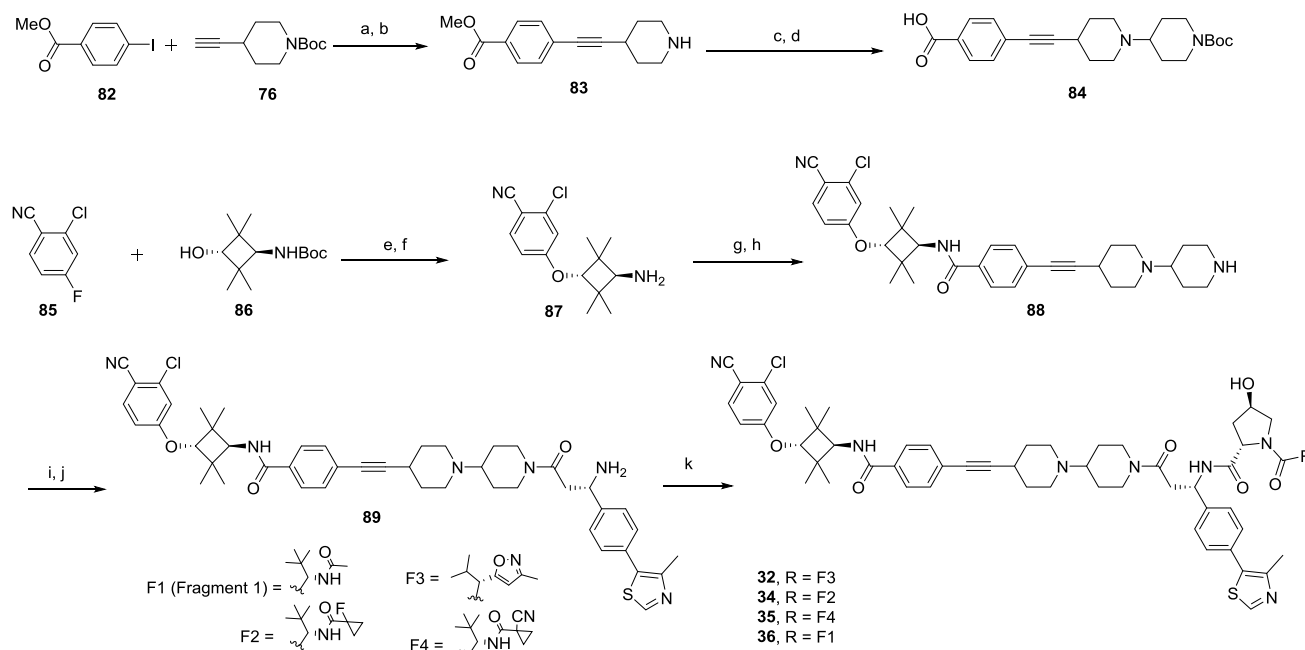
(4*R*)-1-((*S*)-2-(3-(4-(3-(4-Cyano-3-(trifluoromethyl)phenyl)-5,5-dimethyl-4-oxo-2-thioxoimidazolidin-1-yl)-2-fluorobenzamido)propanamido)-3,3-dimethylbutanoyl)-4-hydroxy-*N*-(4-(4-methylthiazol-5-yl)benzyl)pyrrolidine-2-carboxamide (**8**). ¹H NMR (400 MHz, MeOD-*d*₄) δ = 8.94 (s, 1H), 8.16 (d, *J* = 7.2 Hz, 2H), 7.99 (d, *J* = 8.4 Hz, 1H), 7.52–7.31 (m, 6H), 4.63 (s, 1H), 4.59–4.45 (m, 3H), 4.36 (d, *J* = 15.2 Hz, 1H), 3.90 (d, *J* = 10.0 Hz, 1H), 3.83–3.75 (m, 1H), 3.40 (t, *J* = 7.0 Hz, 2H), 2.49 (s, 3H), 2.44–2.00 (m, 4H), 1.60 (s, 6H), 1.04 (s, 9H). UPLC–MS calcd for C₄₃H₄₇F₄N₈O₆S₂ [M + H]⁺: 935.30, found: 935.52. UPLC-retention time: 4.77 min.

(4*R*)-1-((*S*)-2-(4-(3-(4-Cyano-3-(trifluoromethyl)phenyl)-5,5-dimethyl-4-oxo-2-thioxoimidazolidin-1-yl)-2-fluorobenzamido)butanamido)-3,3-dimethylbutanoyl)-4-hydroxy-*N*-(4-(4-methylthiazol-5-yl)benzyl)pyrrolidine-2-carboxamide (**9**). ¹H NMR (400 MHz, MeOD-*d*₄) δ = 8.93 (s, 1H), 8.16 (d, *J* = 7.6 Hz, 2H), 7.99 (d, *J* = 8.0 Hz, 1H), 7.50–7.32 (m, 6H), 4.63 (s, 1H), 4.61–4.45 (m, 3H), 4.35 (d, *J* = 15.6 Hz, 1H), 3.91 (d, *J* = 10.0 Hz, 1H), 3.83–3.55 (m, 3H), 3.41 (t, *J* = 7.2 Hz, 2H), 2.48 (s, 3H), 2.33–2.15 (m, 3H), 2.12–2.00 (m, 3H), 1.60 (s, 6H), 1.04 (s, 9H). UPLC–MS calcd for C₄₆H₄₉F₄N₈O₆S₂ [M + H]⁺: 949.32, found: 949.58 (H⁺). UPLC-retention time: 4.92 min.

(4*R*)-1-((*S*)-2-(5-(4-(3-(4-Cyano-3-(trifluoromethyl)phenyl)-5,5-dimethyl-4-oxo-2-thioxoimidazolidin-1-yl)-2-fluorobenzamido)pentanamido)-3,3-dimethylbutanoyl)-4-hydroxy-*N*-(4-(4-methylthiazol-5-yl)benzyl)pyrrolidine-2-carboxamide (**10**). ¹H NMR (400 MHz, MeOD-*d*₄) δ = 8.97 (s, 1H), 8.16 (d, *J* = 7.4 Hz, 2H), 7.99 (d, *J* = 8.4 Hz, 1H), 7.84 (dd, *J* = 8.0 Hz, *J* = 7.6 Hz, 1H), 7.53–7.39 (m, 4H), 7.38–7.37 (m, 2H), 4.63 (s, 1H), 4.60–4.46 (m, 3H), 4.36 (d, *J* = 15.2 Hz, 1H), 3.90 (d, *J* = 10.8 Hz, 1H), 3.83–3.75 (m, 1H), 3.40 (t, *J* = 7.0 Hz, 2H), 2.51 (s, 3H), 2.38–2.15 (m, 3H), 2.13–2.02 (m, 1H), 1.69–1.55 (m, 10H), 1.04 (s, 9H). UPLC–MS calcd for C₄₇H₅₁F₄N₈O₆S₂ [M + H]⁺: 963.33, found: 963.54. UPLC-retention time: 5.15 min.

Scheme 5. Compounds 29 and 30^a

^aReaction conditions: (a) CuI, PdCl₂(PPh₃)₂, DMF/TEA, 100 °C; (b) reflux; (c) DMF, 80 °C; (d) MeOH, 2 N HCl, reflux; (e) TFA, DCM, rt; (f) K₂CO₃, KI, CH₃CN, reflux; (g) TFA, DCM, rt; (h) HATU, DIPEA, DMF, rt; (i) TFA, DCM, rt; (j) HATU, DIPEA, DMF, rt.

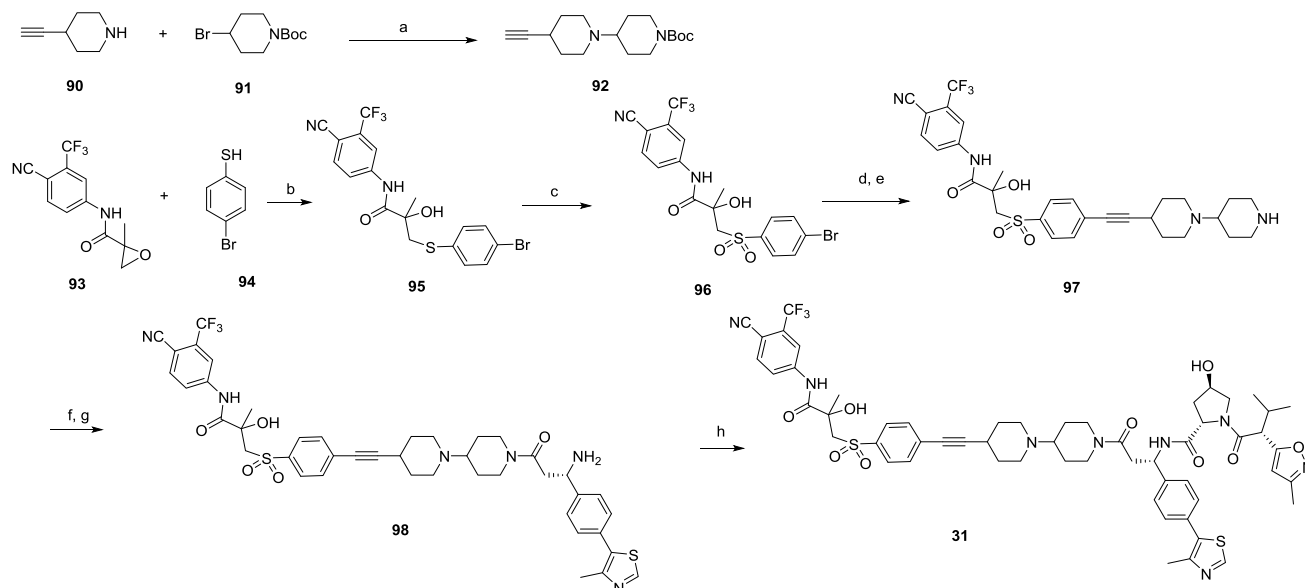
Scheme 6. Compounds 32 and 34–36^a

^aReaction conditions: (a) CuI, PdCl₂(PPh₃)₂, DMF/TEA, 100 °C; (b) TFA, DCM, rt; (c) K₂CO₃, KI, CH₃CN, reflux; (d) NaOH, MeOH/H₂O, rt; (e) NaH, DMF, rt; (f) TFA, DCM, rt; (g) HATU, DIPEA, DMF, rt; (h) TFA, DCM, rt; (i) HATU, DIPEA, DMF, rt; (j) TFA, DCM, rt; (k) HATU, DIPEA, DMF, rt.

(4*R*)-1-((*S*)-2-(6-(4-(3-(4-Cyano-3-(trifluoromethyl)phenyl)-5,5-dimethyl-4-oxo-2-thioxoimidazolidin-1-yl)-2-fluorobenzamido)-hexanamido)-3,3-dimethylbutanoyl)-4-hydroxy-*N*-(4-(4-methylthiazol-5-yl)benzyl)pyrrolidine-2-carboxamide (**11**). ¹H NMR (400 MHz, MeOD-*d*₄) δ = 9.20 (s, 1H), 8.16 (d, *J* = 7.2 Hz, 2H), 7.99 (d, *J* = 8.4 Hz, 1H), 7.83 (dd, *J* = 8.0 Hz, *J* = 8.0 Hz, 1H), 7.52–7.40 (m, 4H), 7.35 (dd, *J* = 7.6 Hz, *J* = 8.0 Hz, 2H), 4.63 (s, 1H), 4.59–4.45 (m, 3H), 4.36 (d, *J* = 15.6 Hz, 1H), 3.90 (d, *J* = 10.4 Hz, 1H), 3.83–3.75 (m, 1H), 3.41 (t, *J* = 6.4 Hz, 2H), 2.51 (s, 3H), 2.38–2.15 (m, 3H), 2.13–2.02

(m, 1H), 1.69–1.55 (m, 10H), 1.49–1.26 (m, 2H), 1.03 (s, 9H). UPLC–MS calcd for C₄₈H₅₃F₄N₈O₆S₂ [M + H]⁺: 991.35, found: 977.52. UPLC-retention time: 5.38 min.

(4*R*)-1-((*S*)-2-(7-(4-(3-(4-Cyano-3-(trifluoromethyl)phenyl)-5,5-dimethyl-4-oxo-2-thioxoimidazolidin-1-yl)-2-fluorobenzamido)-heptanamido)-3,3-dimethylbutanoyl)-4-hydroxy-*N*-(4-(4-methylthiazol-5-yl)benzyl)pyrrolidine-2-carboxamide (**12**). ¹H NMR (400 MHz, MeOD-*d*₄) δ = 9.38 (s, 1H), 8.16 (d, *J* = 7.2 Hz, 2H), 7.99 (d, *J* = 8.4 Hz, 1H), 7.82 (dd, *J* = 8.0 Hz, *J* = 7.6 Hz, 1H), 7.54–7.40 (m, 4H),

Scheme 7. Compound 31^a

^aReaction conditions: (a) CuI, PdCl₂(PPh₃)₂, DMF/TEA, 100 °C; (b) NaH, THF, rt; (c) H₂O₂, (CF₃CO)₂O; (d) CuI, PdCl₂(PPh₃)₂, DMF/TEA, 100 °C; (e) TFA, DCM, rt; (f) HATU, DIPEA, DMF, rt; (g) TFA, DCM, rt; (h) HATU, DIPEA, DMF, rt.

7.40–7.30 (m, 2H), 4.63 (s, 1H), 4.61–4.47 (m, 3H), 4.37 (d, *J* = 15.6 Hz, 1H), 3.91 (d, *J* = 11.2 Hz, 1H), 3.83–3.77 (m, 1H), 3.40 (t, *J* = 7.2 Hz, 2H), 2.53 (s, 3H), 2.35–2.24 (m, 3H), 2.12–2.05 (m, 1H), 1.69–1.55 (m, 10H), 1.46–1.34 (m, 4H), 1.03 (s, 9H). UPLC–MS calcd for C₄₉H₅₅F₄N₈O₆S₂ [M + H]⁺: 991.36, found: 991.53. UPLC-retention time: 5.55 min.

(4*R*)-1-((*S*)-2-(8-(4-(3-(4-Cyano-3-(trifluoromethyl)phenyl)-5,5-dimethyl-4-oxo-2-thioxoimidazolidin-1-yl)-2-fluorobenzamido)-octanamido)-3,3-dimethylbutanoyl)-4-hydroxy-*N*-(4-(4-methylthiazol-5-yl)benzyl)pyrrolidine-2-carboxamide (13). ¹H NMR (400 MHz, MeOD-*d*₄) δ = 9.24 (s, 1H), 8.16 (d, *J* = 7.6 Hz, 2H), 7.99 (d, *J* = 8.4 Hz, 1H), 7.82 (dd, *J* = 8.0 Hz, *J* = 7.6 Hz, 1H), 7.54–7.40 (m, 4H), 7.39–7.30 (m, 2H), 4.64 (s, 1H), 4.62–4.46 (m, 3H), 4.36 (d, *J* = 15.2 Hz, 1H), 3.90 (d, *J* = 10.8 Hz, 1H), 3.83–3.55 (m, 3H), 3.40 (t, *J* = 7.0 Hz, 2H), 2.51 (s, 3H), 2.35–2.17 (m, 3H), 2.12–2.01 (m, 1H), 1.68–1.54 (m, 10H), 1.47–1.32 (m, 6H), 1.02 (s, 9H). UPLC–MS calcd for C₅₀H₅₇F₄N₈O₆S₂ [M + H]⁺: 1005.38, found: 1005.57. UPLC-retention time: 5.74 min.

(4*R*)-1-((*S*)-2-(9-(4-(3-(4-Cyano-3-(trifluoromethyl)phenyl)-5,5-dimethyl-4-oxo-2-thioxoimidazolidin-1-yl)-2-fluorobenzamido)-nonanamido)-3,3-dimethylbutanoyl)-4-hydroxy-*N*-(4-(4-methylthiazol-5-yl)benzyl)pyrrolidine-2-carboxamide (14). ¹H NMR (400 MHz, MeOD-*d*₄) δ = 8.97 (s, 1H), 8.16 (d, *J* = 8.0 Hz, 2H), 7.98 (d, *J* = 8.0 Hz, 1H), 7.82 (dd, *J* = 8.0 Hz, *J* = 7.6 Hz, 1H), 7.49–7.38 (m, 4H), 7.40–7.30 (m, 2H), 4.64 (s, 1H), 4.61–4.47 (m, 3H), 4.35 (d, *J* = 15.6 Hz, 1H), 3.91 (d, *J* = 10.8 Hz, 1H), 3.83–3.75 (m, 1H), 3.40 (t, *J* = 7.2 Hz, 2H), 2.48 (s, 3H), 2.35–2.15 (m, 3H), 2.13–2.05 (m, 1H), 1.67–1.56 (m, 10H), 1.45–1.30 (m, 8H), 1.03 (s, 9H). UPLC–MS calcd for C₅₁H₅₉F₄N₈O₆S₂ [M + H]⁺: 1019.39, found: 1019.42. UPLC-retention time: 5.93 min.

(4*R*)-1-((*S*)-2-(10-(4-(3-(4-Cyano-3-(trifluoromethyl)phenyl)-5,5-dimethyl-4-oxo-2-thioxoimidazolidin-1-yl)-2-fluorobenzamido)-decanamido)-3,3-dimethylbutanoyl)-4-hydroxy-*N*-(4-(4-methylthiazol-5-yl)benzyl)pyrrolidine-2-carboxamide (15). ¹H NMR (400 MHz, MeOD-*d*₄) δ = 8.90 (s, 1H), 8.16 (d, *J* = 7.6 Hz, 2H), 8.03–7.94 (m, 1H), 7.85–7.78 (m, 1H), 7.50–7.30 (m, 6H), 4.63 (s, 1H), 4.61–4.47 (m, 3H), 4.35 (d, *J* = 15.2 Hz, 1H), 3.90 (d, *J* = 11.6 Hz, 1H), 3.83–3.77 (m, 1H), 3.40 (t, *J* = 7.0 Hz, 2H), 2.47 (s, 3H), 2.32–2.18 (m, 3H), 2.14–2.03 (m, 1H), 1.70–1.55 (m, 10H), 1.47–1.25 (m, 10H), 1.03 (s, 9H). UPLC–MS calcd for C₅₂H₆₁F₄N₈O₆S₂ [M + H]⁺: 1033.41, found: 1033.41. UPLC-retention time: 6.15 min.

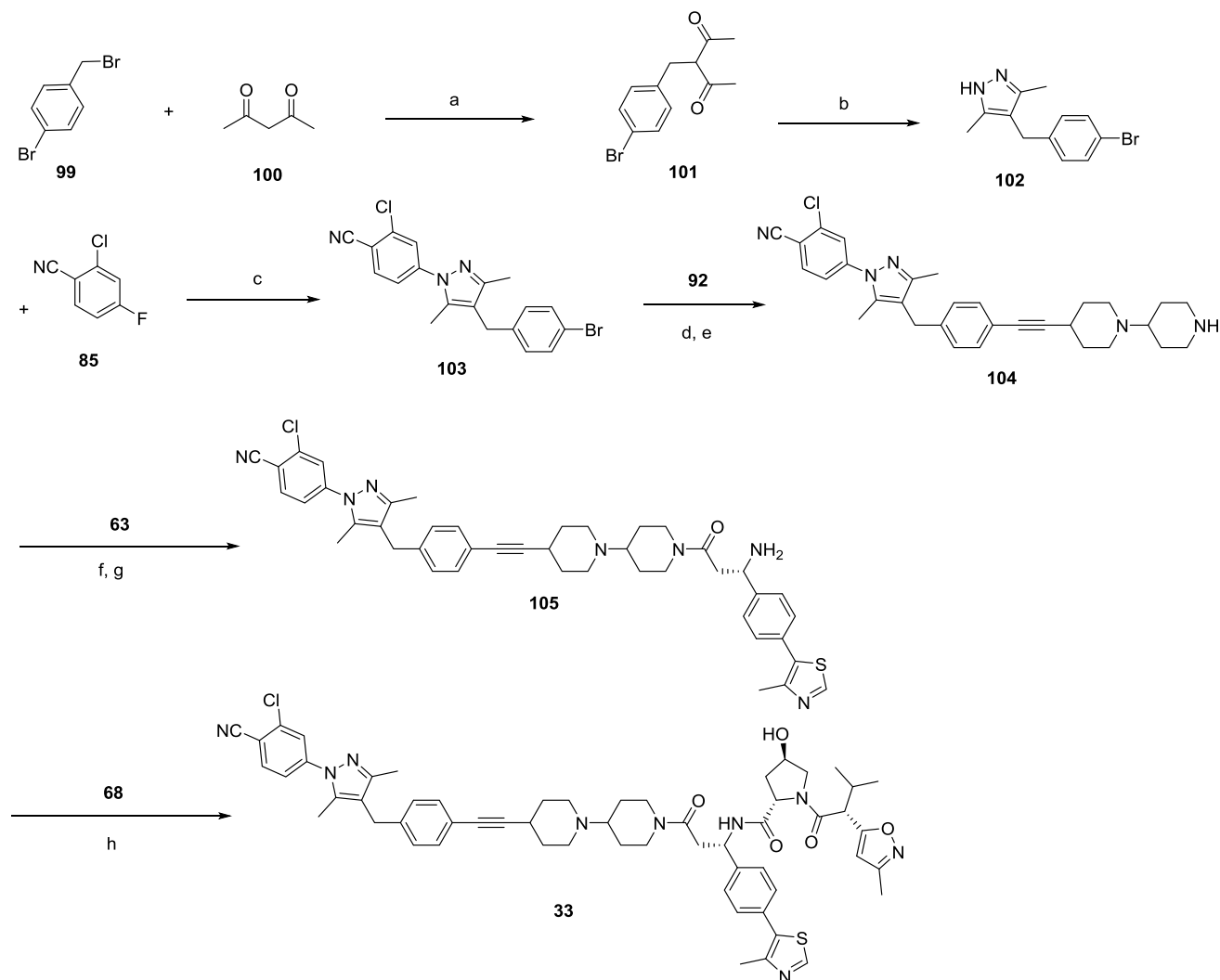
(4*R*)-1-((*S*)-2-(11-(4-(3-(4-Cyano-3-(trifluoromethyl)phenyl)-5,5-dimethyl-4-oxo-2-thioxoimidazolidin-1-yl)-2-fluorobenzamido)-undecanamido)-3,3-dimethylbutanoyl)-4-hydroxy-*N*-(4-(4-methylthiazol-5-yl)benzyl)pyrrolidine-2-carboxamide (16). ¹H NMR (400 MHz, MeOD-*d*₄) δ = 8.98 (s, 1H), 8.15 (d, *J* = 8.4 Hz, 2H), 8.03–7.94 (m, 1H), 7.87–7.75 (m, 1H), 7.49–7.35 (m, 4H), 7.36–7.31 (m, 2H), 4.63 (s, 1H), 4.60–4.46 (m, 3H), 4.35 (d, *J* = 15.6 Hz, 1H), 3.90 (d, *J* = 11.2 Hz, 1H), 3.83–3.55 (m, 3H), 3.39 (t, *J* = 7.0 Hz, 2H), 2.48 (s, 3H), 2.32–2.16 (m, 3H), 2.13–2.04 (m, 1H), 1.68–1.54 (m, 10H), 1.46–1.30 (m, 12H), 1.03 (s, 9H). UPLC–MS calcd for C₅₃H₆₃F₄N₈O₆S₂ [M + H]⁺: 1047.42, found: 1047.43. UPLC-retention time: 6.38 min.

(4*R*)-1-((*S*)-2-(12-(4-(3-(4-Cyano-3-(trifluoromethyl)phenyl)-5,5-dimethyl-4-oxo-2-thioxoimidazolidin-1-yl)-2-fluorobenzamido)-dodecanamido)-3,3-dimethylbutanoyl)-4-hydroxy-*N*-(4-(4-methylthiazol-5-yl)benzyl)pyrrolidine-2-carboxamide (17). ¹H NMR (400 MHz, MeOD-*d*₄) δ = 9.30 (s, 1H), 8.20–8.12 (m, 2H), 8.00 (dd, *J* = 8.3, 1.7 Hz, 1H), 7.85 (t, *J* = 8.0 Hz, 1H), 7.54–7.45 (m, 4H), 7.40–7.34 (m, 2H), 4.65 (s, 1H), 4.57 (dt, *J* = 24.3, 10.3 Hz, 3H), 4.38 (d, *J* = 15.6 Hz, 1H), 3.93 (d, *J* = 11.1 Hz, 1H), 3.82 (dd, *J* = 11.0, 3.8 Hz, 1H), 3.42 (t, *J* = 7.0 Hz, 2H), 2.54 (d, *J* = 3.4 Hz, 3H), 2.41–2.17 (m, 4H), 2.09 (ddd, *J* = 19.6, 10.0, 5.4 Hz, 1H), 1.67–1.62 (m, 3H), 1.61 (s, 6H), 1.36 (d, *J* = 24.1 Hz, 14H), 1.05 (s, 9H). UPLC–MS calcd for C₅₄H₆₅F₄N₈O₆S₂ [M + H]⁺: 1061.44, found: 1061.40. UPLC-retention time: 6.5 min.

General Procedure for Synthesis of Compound 18. DIPEA (5 equiv) and HATU (1.2 equiv) were added to a solution of compound 50 (45.1 mg, 0.1 mmol) and *tert*-butyl 3-(2-(2-aminoethoxy)ethoxy)propanoate (1.1 equiv) in DMF (2 mL). After 30 min at rt, the mixture was subject to HPLC purification to afford the *tert*-butyl protected compound (53) in 92% yield. Then, compound 53 was obtained by a deprotection reaction in TFA/DCM solvent.

DIPEA (5 equiv) and HATU (1.2 equiv) were added to a solution of 53 (48.8 mg, 0.08 mmol) and 49a (1.1 equiv) in DMF (2 mL). After 30 min at rt, the mixture was subject to HPLC purification to afford compound 18 in 85% yield.

(4*R*)-1-((*S*)-13-(*tert*-Butyl)-1-(4-(3-(4-cyano-3-(trifluoromethyl)phenyl)-5,5-dimethyl-4-oxo-2-thioxoimidazolidin-1-yl)-2-fluorophenyl)-1,11-dioxo-5,8-dioxo-2,12-diazatetradecan-14-oyl)-4-hydroxy-*N*-(4-(4-methylthiazol-5-yl)benzyl)pyrrolidine-2-carboxamide (18). ¹H NMR (400 MHz, MeOD-*d*₄) δ = 9.76 (s, 1H), 8.16 (d, *J* = 8.4 Hz, 2H), 7.99 (d, *J* = 8.4 Hz, 1H), 7.86 (dd, *J* = 8.4 Hz, *J* = 8.0 Hz, 1H), 7.57–7.45 (m, 4H), 7.41–7.31 (m, 2H), 4.65 (s, 1H), 4.60–4.46 (m, 3H), 4.36 (d, *J* = 15.6 Hz, 1H), 3.92–3.56 (m, 12H), 2.57 (s, 3H), 2.58–2.41 (m, 2H), 2.22–2.00 (m, 2H), 1.59 (s, 6H), 1.39–1.32 (m,

Scheme 8. Compound 33^a

^aReaction conditions: (a) Na₂CO₃, acetone, reflux; (b) NH₂NH₂, EtOH, reflux; (c) NaH, DMF, rt; (d) CuI, PdCl₂(PPh₃)₂, DMF/TEA, 100 °C; (e) TFA, DCM, rt; (f) HATU, DIPEA, DMF, rt; (g) TFA, DCM, rt; (h) HATU, DIPEA, DMF, rt.

3H), 1.02 (s, 9H). UPLC–MS calcd for C₄₉H₅₅F₄N₈O₈S₂ [M + H]⁺: 1023.35, found 1023.50. UPLC-retention time: 5.2 min.

General Procedure for Synthesis of Compound 19. *n*-BuLi (1 equiv) was added to a solution of compound 56 (2.5 g, 10 mmol) in THF at –78 °C. Then, compound 55 (1 equiv) in THF was added at –78 °C slowly. After 2 h at rt, the reaction mixture was quenched with ice/H₂O and extracted with DCM. The organic layer was separated, washed with brine, dried, and evaporated. The final compound 57 was obtained by flash column chromatography (hexane/EtOAc = 2:1) in 70% yield.

Compound 57 was placed in a 25 mL round-bottom flask (2.7 g, 7 mmol) with 4-iodoaniline (1 equiv), CuI (0.2 equiv), and PdCl₂(PPh₃)₂ (0.1 equiv) in DMF and TEA under Ar. Then, the mixture was stirred for 4 h at 100 °C. After this time, H₂O was added into the resulting complex, which was extracted with EtOAc three times. The organic layer was again washed with H₂O before being dried over MgSO₄, and the solvent was removed under vacuum, leaving the crude product. The pure product 58 was obtained by flash column chromatography (hexane/EtOAc = 4:1) in 80% yield.

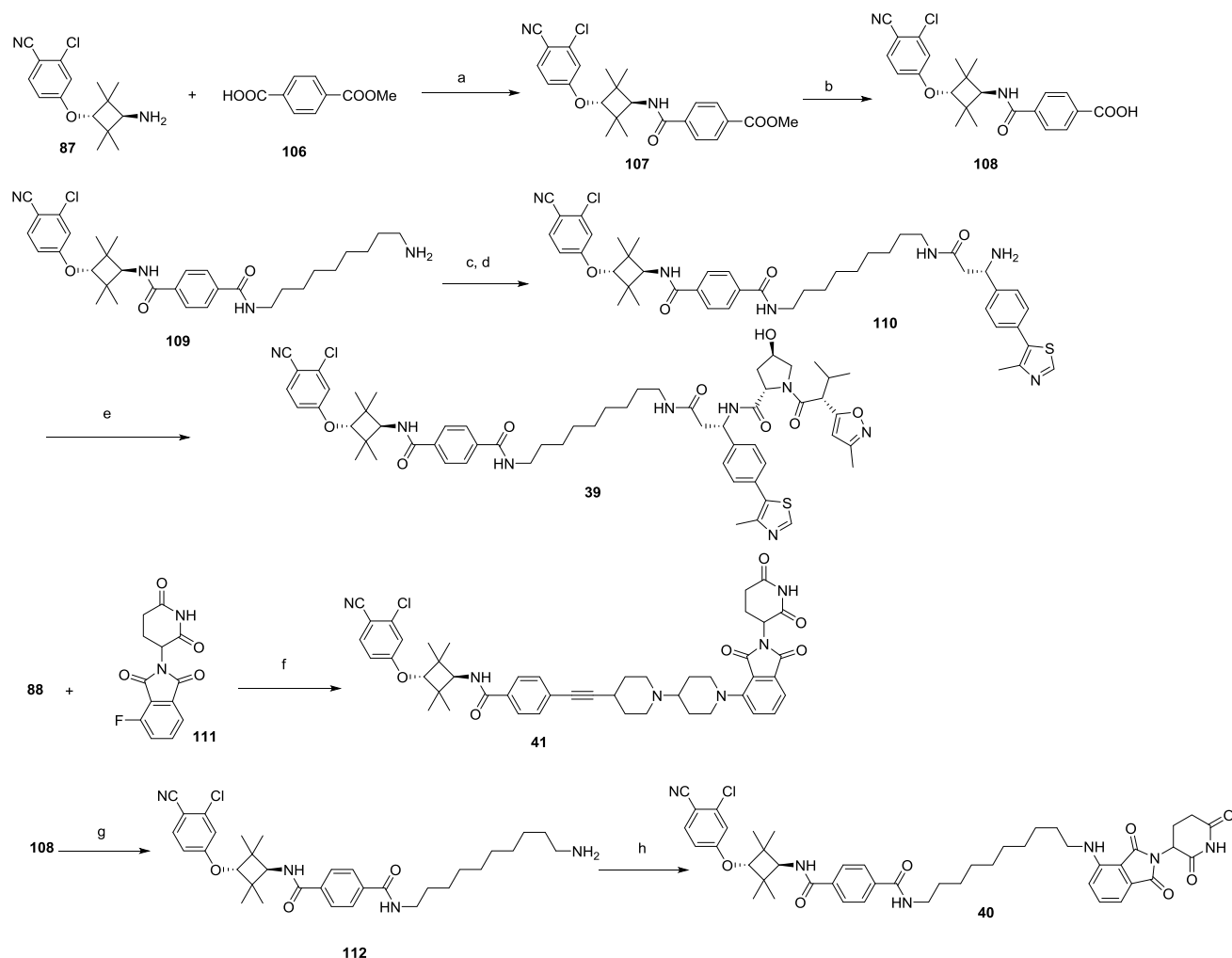
A solution of compound 58 (2.1 g, 5.6 mmol) in 2-hydroxy-2-methylpropanenitrile was refluxed for 8 h. The intermediate 59 was obtained by removing the solvent under reduced pressure and used in the next step without further purification.

A solution of compound 59 (2.2 g, 5 mmol) and 4-isothiocyanato-2-(trifluoromethyl)-benzonitrile (1.1 equiv) in 20 mL of DMF was stirred at 80 °C for 8 h. Then, 10 mL of MeOH and 10 mL of 2 N HCl were added and the mixture was refluxed for another 4 h. After UPLC–MS demonstrated the full conversion of starting materials, the reaction mixture was cooled to rt and H₂O was added into the mixture. The aqueous layer was extracted with EtOAc, and the combined organic layers were washed with brine, then dried over anhydrous Na₂SO₄. The solvent was removed on a rotary evaporator, and the residue was purified by flash column chromatography to afford compound 60 in 60% yield.

A solution of compound 60 in 1:1 TFA/DCM was stirred at rt for 30 min. The solvents were evaporated under reduced pressure to give the corresponding deprotected intermediate 61 (TFA salt) that was used in the following reactions without further purification (95% yield).

DIPEA (5 equiv) and HATU (1.2 equiv) were added to a solution of 61 (62 mg, 0.1 mmol) and compound 49a (1.1 equiv) in DMF (2 mL). After 30 min at rt, the mixture was subject to HPLC purification to afford compound 19 in 90% yield.

(4*R*)-1-((*S*)-2-(7-(5-((4-(3-(4-Cyano-3-(trifluoromethyl)phenyl)-5,5-dimethyl-4-oxo-2-thioxoimidazolidin-1-yl)phenyl)ethynyl)pyridin-2-yl)heptanamido)-3,3-dimethylbutanoyl)-4-hydroxy-*N*-(4-(4-methylthiazol-5-yl)benzyl)pyrrolidine-2-carboxamide (19). ¹H NMR (400 MHz, MeOD-*d*₄) δ 8.97 (s, 1H), 8.37–8.33 (m, 1H), 8.24–8.14 (m, 3H), 8.02 (dd, *J* = 8.3, 2.0 Hz, 1H), 7.75 (dd, *J* = 8.8, 2.3

Scheme 9. Compounds 39–41^a

^aReaction conditions: (a) HATU, DIPEA, DMF, rt; (b) NaOH, H₂O/MeOH, rt; (c) HATU, DIPEA, DMF, rt; (d) TFA, DCM, rt; (e) HATU, DIPEA, DMF, rt; (f) TEA, dimethyl sulfoxide (DMSO), 100 °C; (g) HATU, DIPEA, DMF, rt; (h) HATU, DIPEA, DMF, rt.

Hz, 1H), 7.67 (dd, *J* = 9.1, 2.5 Hz, 2H), 7.51–7.42 (m, 7H), 6.95 (d, *J* = 8.9 Hz, 1H), 4.61–4.53 (m, 3H), 4.39 (d, *J* = 15.6 Hz, 1H), 3.96 (d, *J* = 11.0 Hz, 1H), 3.87–3.82 (m, 1H), 3.70–3.57 (m, 2H), 3.21 (d, *J* = 7.6 Hz, 3H), 2.72 (s, 5H), 2.49 (d, *J* = 2.2 Hz, 3H), 2.41 (t, *J* = 6.7 Hz, 2H), 2.29–2.21 (m, 1H), 2.12 (td, *J* = 9.1, 4.6 Hz, 1H), 1.82–1.74 (m, 3H), 1.60 (s, 6H), 1.08 (s, 9H). UPLC–MS calcd for C₅₅H₅₈F₃N₈O₅S₂ [M + H]⁺: 1031.39, found 1031.48. UPLC-retention time: 5.1 min.

General Procedure for Synthesis of Compounds 20–24. A solution of **61** (3.43 g, 10 mmol), 4-methylthiazole (2 equiv), KOAc (2 equiv), and Pd(OAc)₂ (1%) in DMF/TEA was stirred at 80 °C for 4 h. After the reaction was complete, the TEA was removed under reduced pressure, then H₂O was added into the mixture, and the mixture was extracted three times by EtOAc. The solvent was collected, dried with Na₂SO₄, and evaporated under reduced pressure to give the corresponding intermediate **63** by flash column chromatography (hexane/EtOAc = 4:1) in 80% yield.

To a solution of **64** (1.41 mg, 10 mmol) in MeOH was added H₂SO₄ (1 equiv). Then, the mixture was stirred at 70 °C for 4 h. The mixture was quenched with H₂O and extracted with EtOAc three times. The organic layer was washed with H₂O and brine and dried with Na₂SO₄. The product **65** was obtained by removing the solvent and used without further purification.

t-BuOK (1.5 equiv) was added slowly to a solution of **65** (1.55 g, 10 mmol) in THF, then 2-iodopropane (1.3 equiv) was added dropwise at 0 °C. After the addition was completed, the mixture was stirred at rt overnight. After UPLC–MS demonstrated the full conversion of the

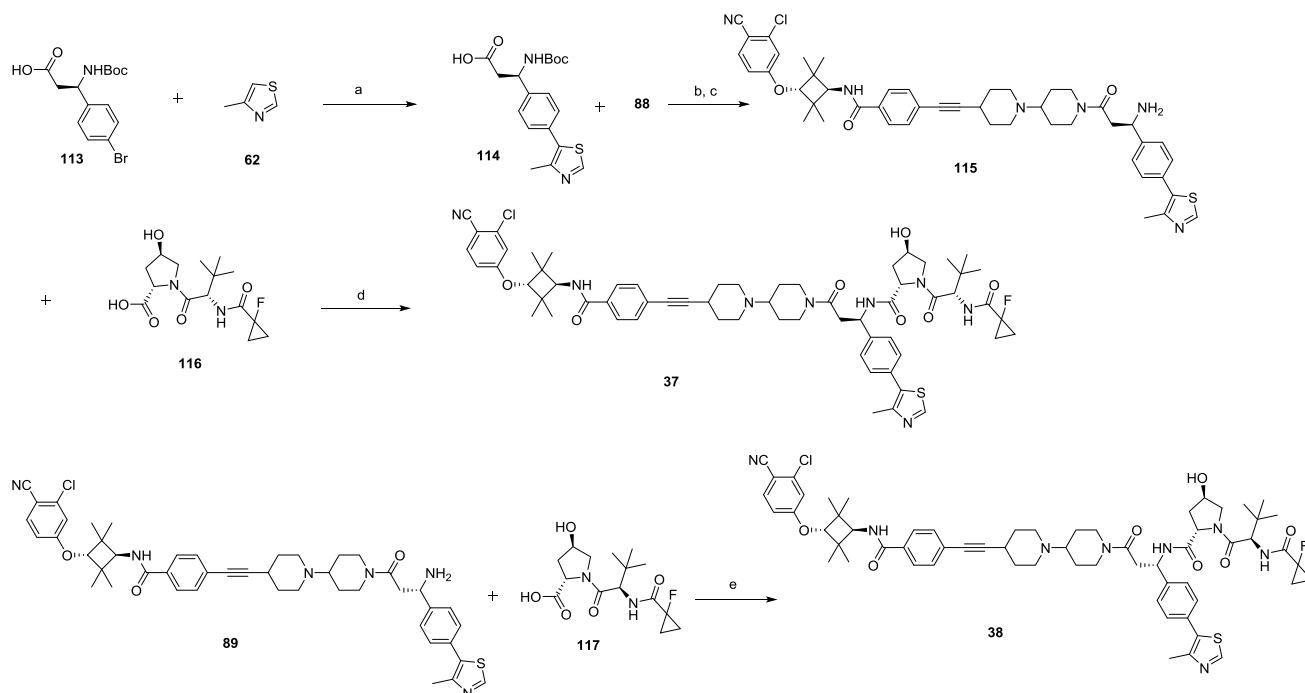
starting materials, the solvent was removed on a rotary evaporator and the residue was purified by flash column chromatography (hexane/EtOAc = 6:1). The desired intermediate **66** was obtained through the hydrolysis by LiOH in THF/H₂O (82% yield).

DIPEA (6 equiv) and HATU (1.2 equiv) were added to a solution of **66** (1.46 g, 8 mmol) and benzyl (2*S*,4*R*)-4-hydroxypiperidine-2-carboxylate hydrochloride (1.1 equiv) in DMF. The mixture was stirred at rt overnight and then the desired intermediate **70** was isolated according to a published method.⁴⁰

Pd–C (10%) was added under H₂ to a solution of **67** (386 mg, 1 mmol) in MeOH and stirred at rt for 2 h. Then, the solvent was removed to afford the product **68** without further purification.

Compound **69** (1.17 g, 10 mmol), **70** (1 equiv), CuI (0.2 equiv), and PdCl₂(PPh₃)₂ (0.1 equiv) in DMF and TEA solvent were placed in a 25 mL round-bottom flask under Ar. Then, the mixture was stirred for 4 h at 100 °C. After this time, H₂O was added into the resulting complex and extracted with EtOAc three times. The organic layer was again washed with H₂O before being dried over MgSO₄, and the solvent was removed under vacuum leaving the crude product. The pure product **71** was obtained by flash column chromatography (hexane/EtOAc = 4:1) in 30% yield.

A solution of **71** and *tert*-butyl 4-((4-aminophenyl)ethynyl)-piperidine-1-carboxylate (1.1 g, 3 mmol) in 2-hydroxy-2-methylpropanenitrile was refluxed for 8 h. The intermediate (**72**) was obtained by removing the solvent under reduced pressure and was used in the next step without further purification.

Scheme 10. Compounds 37–38^a

^aReaction conditions: (a) Pd(OAc)₂, KOAc, 90 °C; (b) HATU, DIPEA, DMF, rt; (c) TFA, DCM, rt; (d) HATU, DIPEA, DMF, rt; (e) HATU, DIPEA, DMF, rt.

A solution of **72** (1.3 g, 3 mmol) and 4-isothiocyanato-2-(trifluoromethyl)benzonitrile (1.1 equiv) in 20 mL of DMF was stirred at 80 °C for 8 h. Then, 10 mL of MeOH and 10 mL of 2 N HCl were added and the mixture was refluxed for another 4 h. After UPLC–MS demonstrated the full conversion of the starting materials, the reaction mixture was cooled to rt and H₂O was added into the mixture. The aqueous layer was extracted with EtOAc, and the combined organic layers were washed with brine and then dried over anhydrous Na₂SO₄. The solvent was removed on a rotary evaporator, and the residue was purified by flash column chromatography. The desired intermediate (**73**) was isolated in 80% yield by deprotection in TFA/DCM.

K₂CO₃ (1.2 equiv) and KI (0.2 equiv) were added to a solution of the intermediate **73** (57.4 mg, 0.1 mmol) and *tert*-butyl 2-bromoacetate (1.2 equiv) in CH₃CN. After stirring the mixture overnight at 100 °C, the solvents were evaporated under reduced pressure to afford the corresponding crude compound that was purified by flash column chromatography (DCM/MeOH = 20:1). Compound **74** was obtained through deprotection by TFA in DCM (75% yield).

DIPEA (5 equiv) and HATU (1.2 equiv) were added to a solution of **74** (45 mg, 0.075 mmol) and compound **49a** (1.1 equiv) in DMF (2 mL). After 30 min at rt, the mixture was subject to HPLC purification to afford compound **24** in 88% yield. Following the procedures used to prepare **24**, compounds **20–23** with different chain lengths were obtained by the same methods.

(4*R*)-1-((*S*)-2-(4-(4-(5-((4-(3-(4-Cyano-3-(trifluoromethyl)phenyl)-5,5-dimethyl-4-oxo-2-thioxoimidazolidin-1-yl)phenyl)ethynyl)pyridin-2-yl)piperazin-1-yl)butanamido)-3,3-dimethylbutanoyl)-4-hydroxy-*N*-(4-(4-methylthiazol-5-yl)benzyl)pyrrolidine-2-carboxamide (**20**). ¹H NMR (400 MHz, DMSO-*d*₆) δ = 9.0 (s, 1H, CONH), 8.6 (t, *J* = 4.0 Hz, 1H), 8.4 (m, 2H), 8.3 (m, 2H), 8.10 (s, 2H), 7.8 (m, 1H), 7.7 (m, 1H), 7.6 (m, 1H), 7.4 (m, 4H), 7.2 (s, 1H), 7.0 (s, CONH, 1H), 4.5 (d, 1H), 4.4 (d, 1H), 4.3 (m, 4H), 4.2 (m, 2H), 3.2 (m, 3H), 3.1 (m, 3H), 2.7 (m, 1H), 2.4 (s, 3H), 2.3 (m, 1H), 2.1 (m, 1H), 1.9 (m, 3H), 1.5 (s, 6H), 1.5 (s, OH, 1H), 1.3 (m, 2H), 1.2 (m, 1H), 0.9 (s, *t*-butyl, 9H). UPLC–MS calcd for C₅₆H₆₀F₃N₁₀O₅S₂ [M + H]⁺: 1073.41, found 1073.54. UPLC–retention time: 5.0 min.

(4*R*)-1-((*S*)-2-(4-(4-(5-((4-(3-(4-Cyano-3-(trifluoromethyl)phenyl)-5,5-dimethyl-4-oxo-2-thioxoimidazolidin-1-yl)phenyl)ethynyl)pyridin-2-yl)piperazin-1-yl)butanamido)-3,3-dimethylbutanoyl)-4-

hydroxy-*N*-((*S*)-1-(4-(4-methylthiazol-5-yl)phenyl)ethyl)pyrrolidine-2-carboxamide (**21**). ¹H NMR (400 MHz, MeOD-*d*₄) δ 9.00–8.93 (m, 1H), 8.38 (d, *J* = 2.3 Hz, 1H), 8.18 (d, *J* = 8.8 Hz, 2H), 8.02 (dd, *J* = 8.3, 1.9 Hz, 1H), 7.79 (dt, *J* = 8.9, 1.9 Hz, 1H), 7.67 (dd, *J* = 8.5, 5.4 Hz, 2H), 7.50–7.41 (m, 6H), 6.99 (d, *J* = 9.0 Hz, 1H), 5.04 (d, *J* = 6.9 Hz, 1H), 4.61–4.53 (m, 3H), 4.45 (d, *J* = 4.8 Hz, 1H), 3.95 (d, *J* = 10.9 Hz, 1H), 3.78–3.63 (m, 3H), 3.53–3.46 (m, 1H), 3.28–3.14 (m, 5H), 2.70–2.57 (m, 2H), 2.51 (t, *J* = 2.5 Hz, 3H), 2.24–2.16 (m, 1H), 2.14–1.93 (m, 4H), 1.61 (d, *J* = 3.6 Hz, 6H), 1.54 (d, *J* = 6.9 Hz, 3H), 1.39 (dd, *J* = 7.0, 3.6 Hz, 1H), 1.08 (d, *J* = 17.4 Hz, 9H). UPLC–MS calcd for C₅₇H₆₂F₃N₁₀O₅S₂ [M + H]⁺: 1087.43, found 1087.55. UPLC–retention time: 5.2 min.

(2*S*,4*R*)-1-((*S*)-2-(5-(4-(5-((4-(3-(4-Cyano-3-(trifluoromethyl)phenyl)-5,5-dimethyl-4-oxo-2-thioxoimidazolidin-1-yl)phenyl)ethynyl)pyridin-2-yl)piperazin-1-yl)pentanamido)-3,3-dimethylbutanoyl)-4-hydroxy-*N*-((*S*)-1-(4-(4-methylthiazol-5-yl)phenyl)ethyl)pyrrolidine-2-carboxamide (**22**). ¹H NMR (400 MHz, MeOD-*d*₄) δ 9.01 (d, *J* = 2.5 Hz, 1H), 8.37 (d, *J* = 2.3 Hz, 1H), 8.20–8.16 (m, 2H), 8.02 (dd, *J* = 8.3, 2.1 Hz, 1H), 7.82–7.75 (m, 1H), 7.71–7.58 (m, 3H), 7.51–7.41 (m, 7H), 6.99 (d, *J* = 8.9 Hz, 1H), 5.03 (d, *J* = 7.0 Hz, 2H), 4.73–4.52 (m, 4H), 4.47 (s, 1H), 3.93 (d, *J* = 11.1 Hz, 1H), 3.78 (dd, *J* = 11.0, 3.9 Hz, 1H), 3.64 (d, *J* = 12.8 Hz, 1H), 3.52–3.46 (m, 1H), 3.23 (s, 4H), 2.50 (d, *J* = 5.1 Hz, 3H), 2.42 (t, *J* = 6.9 Hz, 2H), 2.22 (dd, *J* = 12.8, 8.3 Hz, 1H), 2.00 (td, *J* = 8.9, 4.6 Hz, 1H), 1.79 (dt, *J* = 27.5, 7.7 Hz, 5H), 1.61 (q, *J* = 2.5 Hz, 6H), 1.53 (d, *J* = 6.9 Hz, 3H), 1.07 (d, *J* = 13.3 Hz, 9H). UPLC–MS calcd for C₅₈H₆₄F₃N₁₀O₅S₂ [M + H]⁺: 1101.45, found 1101.53. UPLC–retention time: 4.9 min.

(4*R*)-1-((*S*)-2-(3-(4-(5-((4-(3-(4-Cyano-3-(trifluoromethyl)phenyl)-5,5-dimethyl-4-oxo-2-thioxoimidazolidin-1-yl)phenyl)ethynyl)pyridin-2-yl)piperazin-1-yl)propanamido)-3,3-dimethylbutanoyl)-4-hydroxy-*N*-((*S*)-1-(4-(4-methylthiazol-5-yl)phenyl)ethyl)pyrrolidine-2-carboxamide (**23**). ¹H NMR (400 MHz, MeOD-*d*₄) δ 8.89 (d, *J* = 9.1 Hz, 1H), 8.53 (d, *J* = 7.5 Hz, 1H), 8.38 (d, *J* = 2.3 Hz, 1H), 8.19 (d, *J* = 1.6 Hz, 2H), 8.02 (dt, *J* = 8.2, 2.2 Hz, 1H), 7.78 (dd, *J* = 8.8, 2.3 Hz, 1H), 7.69–7.66 (m, 2H), 7.44 (dd, *J* = 9.2, 3.0 Hz, 6H), 6.98 (d, *J* = 8.9 Hz, 1H), 5.04 (t, *J* = 7.1 Hz, 1H), 4.57 (d, *J* = 5.3 Hz, 2H), 4.46 (s, 1H), 3.95 (d, *J* = 11.0 Hz, 1H), 3.78–3.71 (m, 2H), 3.63 (d, *J* = 11.2 Hz, 1H), 3.52–3.46 (m, 1H), 3.30–3.15 (m, 5H), 2.60 (t, *J* = 6.3 Hz, 2H), 2.50 (d, *J* = 1.9 Hz, 3H), 2.21 (dd, *J* = 13.1, 7.6 Hz, 1H),

2.09 (t, *J* = 6.9 Hz, 2H), 1.98 (td, *J* = 9.2, 4.6 Hz, 1H), 1.61 (d, *J* = 3.6 Hz, 6H), 1.53 (d, *J* = 7.0 Hz, 3H), 1.39 (dd, *J* = 6.7, 3.5 Hz, 1H), 1.10 (s, 9H). UPLC–MS calcd for C₅₆H₆₀F₃N₁₀O₅S₂ [M + H]⁺: 1073.41, found 1073.49. UPLC-retention time: 4.8 min.

(4*R*)-1-((*S*)-2-(2-(4-(5-((4-(3-(4-Cyano-3-(trifluoromethyl)phenyl)-5,5-dimethyl-4-oxo-2-thioxoimidazolidin-1-yl)phenyl)ethynyl)pyridin-2-yl)piperazin-1-yl)acetamido)-3,3-dimethylbutanoyl)-4-hydroxy-*N*-((*S*)-1-(4-(4-methylthiazol-5-yl)phenyl)ethyl)pyrrolidine-2-carboxamide (24). ¹H NMR (400 MHz, MeOD-*d*₄) δ 10.00–9.92 (m, 1H), 8.36–8.29 (m, 1H), 8.23–8.10 (m, 3H), 8.10–7.96 (m, 2H), 7.74 (dd, *J* = 8.5, 2.6 Hz, 2H), 7.60–7.47 (m, 6H), 7.42 (dd, *J* = 6.6, 3.5 Hz, 1H), 5.07 (d, *J* = 6.3 Hz, 1H), 4.68 (s, 1H), 4.65–4.58 (m, 1H), 4.49 (s, 1H), 4.23–4.05 (m, 4H), 3.95 (d, *J* = 11.0 Hz, 1H), 3.78 (dd, *J* = 11.2, 4.2 Hz, 1H), 3.64 (s, 2H), 3.02 (s, 1H), 2.89 (s, 1H), 2.63 (s, 3H), 2.26 (dd, *J* = 13.2, 7.8 Hz, 1H), 2.06–1.94 (m, 1H), 1.61 (s, 6H), 1.54 (d, *J* = 7.0 Hz, 3H), 1.39 (dd, *J* = 6.7, 3.5 Hz, 3H), 1.09 (d, *J* = 9.9 Hz, 9H). UPLC–MS calcd for C₅₅H₅₈F₃N₁₀O₅S₂ [M + H]⁺: 1059.40, found 1059.45. UPLC-retention time: 5.2 min.

General Procedure for Synthesis of Compound 25. Triphosgene (1 equiv) was added to a solution of compound 49b (44.4 mg, 0.1 mmol) in DCM and DIPEA (4 equiv) at rt. The reaction mixture was stirred at rt for 30 min, and then compound 73 (1 equiv) was added. After an additional 1 h at rt, the mixture was subject to HPLC purification to afford compound 25 in 83% yield.

4-(5-((4-(3-(4-Cyano-3-(trifluoromethyl)phenyl)-5,5-dimethyl-4-oxo-2-thioxoimidazolidin-1-yl)phenyl)ethynyl)pyridin-2-yl)-*N*-((2*S*)-1-((4*R*)-4-hydroxy-2-(((*S*)-1-(4-(4-methylthiazol-5-yl)phenyl)ethyl)carbamoyl)pyrrolidin-1-yl)-3,3-dimethyl-1-oxobutan-2-yl)-piperazine-1-carboxamide (25). ¹H NMR (400 MHz, MeOD-*d*₄) δ 9.01 (s, 1H), 8.29 (d, *J* = 2.3 Hz, 1H), 8.23–8.16 (m, 2H), 8.02 (dd, *J* = 8.3, 2.0 Hz, 1H), 7.92 (dt, *J* = 9.3, 2.5 Hz, 1H), 7.75–7.67 (m, 2H), 7.55 (d, *J* = 8.5 Hz, 1H), 7.50–7.42 (m, 5H), 7.15 (dd, *J* = 9.4, 3.5 Hz, 1H), 6.84 (dd, *J* = 8.5, 2.3 Hz, 1H), 5.04 (d, *J* = 7.0 Hz, 1H), 4.60 (d, *J* = 8.5 Hz, 1H), 4.47 (d, *J* = 4.8 Hz, 1H), 3.95 (d, *J* = 11.2 Hz, 1H), 3.78 (q, *J* = 3.9 Hz, 4H), 3.69 (d, *J* = 5.0 Hz, 3H), 3.65–3.59 (m, 1H), 3.23 (d, *J* = 7.4 Hz, 1H), 2.51 (s, 2H), 2.26–2.18 (m, 1H), 1.99 (ddd, *J* = 13.1, 9.0, 4.4 Hz, 1H), 1.61 (s, 6H), 1.54 (d, *J* = 7.1 Hz, 3H), 1.39 (dd, *J* = 6.7, 3.5 Hz, 3H), 1.20 (t, *J* = 7.1 Hz, 1H), 1.09 (s, 9H). UPLC–MS calcd for C₅₄H₅₆F₃N₁₀O₅S₂ [M + H]⁺: 1045.38, found 1045.42. UPLC-retention time: 6.4 min.

General Procedure for Synthesis of Compound 26. DIPEA (5 equiv) and HATU (1.2 equiv) were added to a solution of compound 50 (45.1 mg, 0.1 mmol) and *tert*-butyl-(9-aminononyl)carbamate (1.1 equiv) in DMF (2 mL). After 30 min at rt, the mixture was subject to HPLC purification to afford Boc protected compound 54 in 90% yield. Then, compound 54 was obtained by a deprotection reaction in TFA/DCM solvent.

DIPEA (5 equiv) and HATU (1.2 equiv) were added to a solution of 54 (47 mg, 0.08 mmol) and 63 (1.1 equiv) in DMF (2 mL). After 30 min at rt, the mixture was subject to HPLC purification to afford compound (S)-*N*-(9-(3-amino-3-(4-(4-methylthiazol-5-yl)phenyl)propanamido)nonyl)-4-(3-(4-cyano-3-(trifluoromethyl)phenyl)-5,5-dimethyl-4-oxo-2-thioxoimidazolidin-1-yl)-2-fluorobenzamide in 80% yield after deprotection in TFA/DCM.

DIPEA (5 equiv) and HATU (1.2 equiv) were added to a solution of (S)-*N*-(9-(3-amino-3-(4-(4-methylthiazol-5-yl)phenyl)propanamido)nonyl)-4-(3-(4-cyano-3-(trifluoromethyl)phenyl)-5,5-dimethyl-4-oxo-2-thioxoimidazolidin-1-yl)-2-fluorobenzamide (66 mg, 0.08 mmol) and 68 (1.1 equiv) in DMF (2 mL). After 30 min at rt, the mixture was subject to HPLC purification to afford compound 26 in 84% yield.

(2*S*,4*R*)-*N*-((*S*)-3-(9-(4-(3-(4-Cyano-3-(trifluoromethyl)phenyl)-5,5-dimethyl-4-oxo-2-thioxoimidazolidin-1-yl)-2-fluorobenzamido)nonyl)amino)-1-(4-(4-methylthiazol-5-yl)phenyl)-3-oxopropyl)-4-hydroxy-1-((*R*)-3-methyl-2-(3-methylisoxazol-5-yl)butanoyl)pyrrolidine-2-carboxamide (26). ¹H NMR (400 MHz, MeOD-*d*₄) δ 9.78 (s, 1H), 8.26–8.15 (m, 2H), 8.02 (dd, *J* = 8.3, 2.0 Hz, 1H), 7.85 (t, *J* = 8.1 Hz, 1H), 7.56 (s, 4H), 7.40 (d, *J* = 10.1 Hz, 1H), 6.24 (s, 1H), 5.37 (dd, *J* = 8.0, 6.0 Hz, 1H), 4.49 (dd, *J* = 17.4, 9.4 Hz, 2H), 3.97–3.71 (m, 2H), 3.67–3.57 (m, 1H), 3.41 (t, *J* = 7.0 Hz, 3H), 3.11 (td, *J* = 6.8, 3.9 Hz, 2H), 3.02 (s, 1H), 2.94–2.69 (m, 3H), 2.60 (s, 3H), 2.43 (q, *J* = 9.4, 8.6 Hz, 1H), 2.27 (s, 2H), 2.18 (t, *J* = 10.8

Hz, 1H), 1.98 (ddd, *J* = 13.1, 8.5, 5.1 Hz, 1H), 1.61 (s, 6H), 1.47–1.33 (m, 6H), 1.25 (d, *J* = 31.7 Hz, 6H), 1.07 (d, *J* = 6.5 Hz, 3H), 0.89 (dd, *J* = 12.4, 6.6 Hz, 3H). UPLC–MS calcd for C₅₆H₆₄F₃N₉O₅S₂ [M + H]⁺: 1114.43, found 1114.49. UPLC-retention time: 6.0 min.

General Procedure for Synthesis of Compounds 27 and 28. K₂CO₃ (1.2 equiv) and KI (0.2 equiv) were added to a solution of the intermediate 73 (57.4 mg, 0.1 mmol) and *tert*-butyl (3-bromopropyl)carbamate (1.2 equiv) in CH₃CN was added. After stirring the mixture overnight at 100 °C, the solvents were evaporated under reduced pressure to afford the corresponding crude compound that was purified by flash column chromatography (DCM/MeOH = 20:1). Then, 4-(3-(4-((6-(4-(3-aminopropyl)piperazin-1-yl)pyridin-3-yl)ethynyl)phenyl)-4,4-dimethyl-5-oxo-2-thioxoimidazolidin-1-yl)-2-(trifluoromethyl)benzotrile was obtained through deprotection by TFA in DCM (72% yield).

DIPEA (5 equiv) and HATU (1.2 equiv) were added to a solution of the compound 4-(3-(4-((6-(4-(3-aminopropyl)piperazin-1-yl)pyridin-3-yl)ethynyl)phenyl)-4,4-dimethyl-5-oxo-2-thioxoimidazolidin-1-yl)-2-(trifluoromethyl)benzotrile (44 mg, 0.07 mmol) and 63 (1.1 equiv) in DMF (2 mL). After 30 min at rt, the mixture was subject to HPLC purification to afford compound (S)-3-amino-*N*-(3-(4-(5-((4-(3-(4-cyano-3-(trifluoromethyl)phenyl)-5,5-dimethyl-4-oxo-2-thioxoimidazolidin-1-yl)phenyl)ethynyl)pyridin-2-yl)piperazin-1-yl)propyl)-3-(4-(4-methylthiazol-5-yl)phenyl)propanamide in 81% yield after deprotection with TFA/DCM.

DIPEA (5 equiv) and HATU (1.2 equiv) were added to a solution of (S)-3-amino-*N*-(3-(4-(5-((4-(3-(4-cyano-3-(trifluoromethyl)phenyl)-5,5-dimethyl-4-oxo-2-thioxoimidazolidin-1-yl)phenyl)ethynyl)pyridin-2-yl)piperazin-1-yl)propyl)-3-(4-(4-methylthiazol-5-yl)phenyl)propanamide (44 mg, 0.05 mmol) and 68 (1.1 equiv) in DMF (2 mL). After 30 min at rt, the mixture was subject to HPLC purification to afford compound 27 in 84% yield. Following the procedures used to prepare compound 27, compound 28 with different chain lengths was obtained with the same methods.

(2*S*,4*R*)-*N*-((*S*)-3-(4-(5-((4-(3-(4-Cyano-3-(trifluoromethyl)phenyl)-5,5-dimethyl-4-oxo-2-thioxoimidazolidin-1-yl)phenyl)ethynyl)pyridin-2-yl)piperazin-1-yl)propyl)amino)-1-(4-(4-methylthiazol-5-yl)phenyl)-3-oxopropyl)-4-hydroxy-1-((*R*)-3-methyl-2-(3-methylisoxazol-5-yl)butanoyl)pyrrolidine-2-carboxamide (27). ¹H NMR (400 MHz, MeOD-*d*₄) δ 9.02–8.94 (m, 1H), 8.38 (t, *J* = 4.2 Hz, 1H), 8.22–8.14 (m, 2H), 8.02 (dd, *J* = 8.2, 2.0 Hz, 1H), 7.79 (td, *J* = 8.4, 2.4 Hz, 1H), 7.73–7.67 (m, 2H), 7.64 (s, 1H), 7.58–7.42 (m, 4H), 6.98 (dd, *J* = 26.1, 8.9 Hz, 1H), 5.44–5.32 (m, 1H), 4.72–4.66 (m, 1H), 4.60 (s, 1H), 4.49 (s, 1H), 3.89 (d, *J* = 11.0 Hz, 1H), 3.77 (dd, *J* = 11.0, 4.2 Hz, 1H), 3.68–3.49 (m, 2H), 3.31–2.83 (m, 7H), 2.53 (d, *J* = 5.3 Hz, 3H), 2.30–2.11 (m, 2H), 2.00 (s, 3H), 1.78 (d, *J* = 8.1 Hz, 2H), 1.66 (d, *J* = 6.6 Hz, 1H), 1.61 (s, 6H), 1.48–1.27 (m, 2H), 1.08 (s, 1H), 1.00 (s, 6H). UPLC–MS calcd for C₆₀H₆₃F₃N₁₁O₆S₂ [M + H]⁺: 1154.44, found 1154.56. UPLC-retention time: 5.6 min.

(2*S*,4*R*)-*N*-((*S*)-3-(4-(5-((4-(((1*r*,3*r*)-3-(3-Chloro-4-cyanophenoxy)-2,2,4,4-tetramethylcyclobutyl)carbamoyl)phenyl)ethynyl)pyridin-2-yl)piperazin-1-yl)-1-(4-(4-methylthiazol-5-yl)phenyl)-3-oxopropyl)-4-hydroxy-1-((*R*)-3-methyl-2-(3-methylisoxazol-5-yl)butanoyl)pyrrolidine-2-carboxamide (28). ¹H NMR (400 MHz, MeOD-*d*₄) δ 9.01 (s, 1H), 8.28 (s, 1H), 7.86 (d, *J* = 7.8 Hz, 3H), 7.75 (d, *J* = 8.7 Hz, 1H), 7.65 (d, *J* = 7.9 Hz, 2H), 7.57–7.41 (m, 4H), 7.16 (s, 1H), 7.10 (d, *J* = 8.2 Hz, 1H), 7.01 (d, *J* = 8.8 Hz, 1H), 6.24 (d, *J* = 28.0 Hz, 1H), 5.45 (d, *J* = 26.8 Hz, 1H), 4.61–4.46 (m, 2H), 4.32 (s, 1H), 4.20 (s, 1H), 3.93–3.87 (m, 1H), 3.80–3.48 (m, 10H), 3.07 (ddd, *J* = 22.9, 19.4, 11.3 Hz, 2H), 2.48 (s, 3H), 2.39 (d, *J* = 6.2 Hz, 1H), 2.26 (d, *J* = 6.0 Hz, 3H), 2.05–1.97 (m, 1H), 1.32 (s, 6H), 1.26 (s, 6H), 1.11–1.02 (m, 3H), 0.92–0.83 (m, 3H). UPLC–MS calcd for C₆₀H₆₅ClN₉O₇S₂ [M + H]⁺: 1090.44, found 1090.56. UPLC-retention time: 6.6 min.

General Procedure for Synthesis of Compounds 29 and 30. Compound 75 (2.19 g, 10 mmol), 76 (1.1 equiv), CuI (0.2 equiv), and PdCl₂(PPh₃)₂ (0.1 equiv) in DMF and TEA were placed in a 25 mL round-bottom flask under Ar. Then, the mixture was stirred for 4 h at 100 °C. After this time, H₂O was added into the resulting complex and extracted with EtOAc three times. The organic layer was again washed with H₂O before being dried over MgSO₄, and the solvent was removed under vacuum leaving the crude product. The pure product (77) was

obtained by flash column chromatography (hexane/EtOAc = 4:1) in 80% yield.

A solution of **77** (2.4 g, 8 mmol) in 2-hydroxy-2-methylpropanenitrile was refluxed for 8 h. Then, by removing the solvent under reduced pressure, the intermediate **78** was obtained and used in the next step without further purification.

A solution of **78** (2.9 g, 8 mmol) and 4-isothiocyanato-2-(trifluoromethyl)benzotrile (1.1 equiv) in 20 mL of DMF was stirred at 80 °C for 8 h. Then, 10 mL of MeOH and 10 mL of 2 N HCl were added and the mixture was refluxed for another 4 h. After UPLC–MS demonstrated the full conversion of starting materials, the reaction mixture was cooled to rt and H₂O was added into the mixture. The aqueous layer was extracted with EtOAc, and the combined organic layers were washed with brine and then dried over anhydrous Na₂SO₄. The solvent was removed on a rotary evaporator, and the residue was purified by flash column chromatography. The desired intermediate **79** was isolated in 85% yield by the deprotection in TFA/DCM.

K₂CO₃ (1.2 equiv) and KI (0.2 equiv) were added to a solution of the intermediate **79** (3 g, 6 mmol) and *tert*-butyl 4-bromopiperidine-1-carboxylate (1.2 equiv) in CH₃CN. After stirring the mixture overnight at 100 °C, the solvents were evaporated under reduced pressure to afford the corresponding crude compound that was purified by flash column chromatography (DCM/MeOH = 20:1). Then, **80** was obtained through the deprotection by TFA in DCM (82% yield).

DIPEA (5 equiv) and HATU (1.2 equiv) were added to a solution of compounds **80** (57.9 mg, 0.1 mmol) and **63** (1.1 equiv) in DMF (2 mL). After 30 min at rt, the mixture was subject to HPLC purification to afford compound **81** in 85% yield after deprotection in TFA/DCM.

DIPEA (5 equiv) and HATU (1.2 equiv) were added to a solution of compounds **81** (70 mg, 0.85 mmol) and **68** (1.1 equiv) in DMF (2 mL). After 30 min at rt, the mixture was subject to HPLC purification to afford compound **29** in 86% yield. Following the procedures used to prepare compound **29**, compound **30** was obtained with the same methods.

(2*S*,4*R*)-*N*-((*S*)-3-(4-((4-(3-(4-Cyano-3-(trifluoromethyl)phenyl)-5,5-dimethyl-4-oxo-2-thioxoimidazolidin-1-yl)phenyl)ethynyl)-[1,4'-bipiperidin]-1'-yl)-1-(4-(4-methylthiazol-5-yl)phenyl)-3-oxopropyl)-4-hydroxy-1-((*R*)-3-methyl-2-(3-methylisoxazol-5-yl)-butanoyl)pyrrolidine-2-carboxamide (**29**). ¹H NMR (400 MHz, MeOD-*d*₄) δ 9.76 (s, 1H), 8.28–8.16 (m, 2H), 8.01 (dt, *J* = 8.2, 2.6 Hz, 1H), 7.88–7.81 (m, 1H), 7.71–7.50 (m, 5H), 7.47–7.35 (m, 1H), 7.10 (dd, *J* = 61.1, 9.5 Hz, 1H), 6.33–6.21 (m, 1H), 5.56–5.32 (m, 2H), 4.70 (s, 1H), 4.57–4.24 (m, 3H), 4.04–3.41 (m, 7H), 3.29–2.85 (m, 7H), 2.75–2.66 (m, 1H), 2.60 (d, *J* = 5.4 Hz, 2H), 2.48–2.31 (m, 2H), 2.30–2.14 (m, 6H), 2.06–1.77 (m, 4H), 1.66–1.44 (m, 6H), 1.41–1.23 (m, 2H), 1.11–0.99 (m, 3H), 0.87 (qd, *J* = 10.6, 9.5, 5.8 Hz, 3H). UPLC–MS calcd for C₅₈H₆₃F₃N₉O₆S₂ [M + H]⁺: 1102.43, found 1102.37. UPLC-retention time: 4.9 min.

(2*S*,4*R*)-*N*-((*S*)-3-(4-((7-(6-Cyano-5-(trifluoromethyl)pyridin-3-yl)-8-oxo-6-thioxo-5,7-diazaspiro[3.4]octan-5-yl)phenyl)ethynyl)-[1,4'-bipiperidin]-1'-yl)-1-(4-(4-methylthiazol-5-yl)phenyl)-3-oxopropyl)-4-hydroxy-1-((*R*)-3-methyl-2-(3-methylisoxazol-5-yl)-butanoyl)pyrrolidine-2-carboxamide (**30**). ¹H NMR (400 MHz, MeOD-*d*₄) δ 9.18 (t, *J* = 2.8 Hz, 1H), 8.93 (s, 1H), 8.66 (t, *J* = 2.9 Hz, 1H), 7.89 (t, *J* = 9.4 Hz, 1H), 7.70 (s, 1H), 7.63 (d, *J* = 7.8 Hz, 1H), 7.58–7.38 (m, 5H), 6.26 (d, *J* = 15.8 Hz, 1H), 5.53–5.33 (m, 3H), 4.57–4.41 (m, 2H), 4.30 (s, 2H), 3.95–3.73 (m, 3H), 3.58 (d, *J* = 28.3 Hz, 5H), 3.26–3.07 (m, 5H), 2.95 (d, *J* = 53.1 Hz, 3H), 2.72 (s, 2H), 2.52 (t, *J* = 5.8 Hz, 3H), 2.27 (d, *J* = 6.9 Hz, 3H), 2.19 (d, *J* = 19.2 Hz, 4H), 1.98 (d, *J* = 15.5 Hz, 2H), 1.63 (s, 2H), 1.39 (dd, *J* = 6.7, 3.4 Hz, 1H), 1.32 (d, *J* = 8.2 Hz, 2H), 1.14–1.02 (m, 3H), 0.94–0.84 (m, 3H). UPLC–MS calcd for C₅₈H₆₃F₃N₁₀O₆S₂ [M + H]⁺: 1115.42, found 1115.49. UPLC-retention time: 5.1 min.

General Procedure for Synthesis of Compounds 31. K₂CO₃ (1.2 equiv) and KI (0.2 equiv) were added to a solution of the intermediate **90** (1 g, 10 mmol) and **91** (1.2 equiv) in CH₃CN. After stirring the mixture overnight at 100 °C, the solvents were evaporated under reduced pressure to afford the corresponding crude compound **92** that was purified by flash column chromatography (DCM/MeOH = 20:1) in 85% yield.

A solution of **94** (1.3 equiv) in THF was added to a mixture of NaH (1.3 equiv) in THF at 0 °C and stirred for 5 min. Then, a solution of **93** (2.7 g, 10 mmol) in THF was added slowly. The mixture was stirred at rt for 3 h. After UPLC–MS demonstrated the full conversion of starting materials, the solvent THF was distilled off and some EtOAc was added and the solution was washed with brine and H₂O. The combined organic layers were dried over anhydrous Na₂SO₄. The solvent was removed on a rotary evaporator giving the desired intermediate **95**, which was used without further purification.

Compound **95** (460 mg, 1 mmol) was dissolved in DCM and 30% H₂O₂ (8 equiv) was added; then, the mixture was cooled to –55 °C and trifluoroacetic anhydride (6 equiv) was added very slowly, keeping the reaction temperature below 0 °C. After the addition was complete, the reaction mixture was stirred at rt for 16 h. After UPLC–MS demonstrated the full conversion of starting materials, ice/H₂O and brine were added into the mixture, which was stirred for another 20 min; then, the organic layer was collected and dried with Na₂SO₄. The solvent was removed on a rotary evaporator giving the desired intermediate **96**, which was purified by flash column chromatography (hexane/EtOAc = 2:1) in 80% yield.

Compounds **96** (390 mg, 0.8 mmol) and **92**, *tert*-butyl 4-ethynyl-[1,4'-bipiperidine]-1'-carboxylate (1.1 equiv), CuI (0.2 equiv), and PdCl₂(PPh₃)₂ (0.1 equiv) in DMF and TEA solvent were placed in a 25 mL round-bottom flask under Ar. Then, the mixture was stirred for 4 h at 100 °C. Then, H₂O was added into the resulting complex, which was extracted with EtOAc three times. The organic layer was again washed with H₂O before being dried over MgSO₄ and the solvent was removed under vacuum leaving the crude product. The pure product was obtained by flash column chromatography (DCM/MeOH = 20:1). Then, compound **97** was obtained through the deprotection by TFA in DCM (82% yield).

DIPEA (5 equiv) and HATU (1.2 equiv) were added to a solution of compounds **97** (60.2 mg, 0.1 mmol) and **63** (1.1 equiv) in DMF (2 mL). After 30 min at rt, the mixture was subject to HPLC purification to afford compound **98** in 88% yield after deprotection in TFA/DCM.

DIPEA (5 equiv) and HATU (1.2 equiv) were added to a solution of compounds **98** (67.7 mg, 0.08 mmol) and **68** (1.1 equiv) in DMF (2 mL). After 30 min at rt, the mixture was subject to HPLC purification to afford compound **31** in 83% yield.

(2*S*,4*R*)-*N*-((1*S*)-3-(4-((4-(3-(4-Cyano-3-(trifluoromethyl)phenyl)-amino)-2-hydroxy-2-methyl-3-oxopropyl)sulfinyl)phenyl)ethynyl)-[1,4'-bipiperidin]-1'-yl)-1-(4-(4-methylthiazol-5-yl)phenyl)-3-oxopropyl)-4-hydroxy-1-((*R*)-3-methyl-2-(3-methylisoxazol-5-yl)-butanoyl)pyrrolidine-2-carboxamide (**31**). ¹H NMR (400 MHz, MeOD-*d*₄) δ 8.93 (s, 1H), 8.61 (dd, *J* = 16.4, 8.6 Hz, 1H), 8.26 (s, 1H), 8.07–7.83 (m, 4H), 7.47 (d, *J* = 28.4 Hz, 5H), 6.31–6.20 (m, 1H), 5.45 (d, *J* = 25.2 Hz, 2H), 4.71 (s, 1H), 4.59–4.41 (m, 2H), 4.29 (s, 2H), 4.12 (dd, *J* = 14.8, 1.7 Hz, 1H), 3.96–3.70 (m, 3H), 3.70–3.44 (m, 6H), 3.27–3.05 (m, 4H), 2.95 (s, 2H), 2.70–2.60 (m, 1H), 2.52 (t, *J* = 5.1 Hz, 3H), 2.39 (d, *J* = 32.8 Hz, 2H), 2.27 (d, *J* = 6.3 Hz, 3H), 2.16 (s, 2H), 2.03–1.89 (m, 2H), 1.79–1.66 (m, 1H), 1.58–1.47 (m, 3H), 1.41–1.27 (m, 2H), 1.12–0.96 (m, 3H), 0.89 (s, 3H). UPLC–MS calcd for C₅₆H₆₄F₃N₉O₇S₂ [M + H]⁺: 1125.42, found 1125.49. UPLC-retention time: 4.0 min.

General Procedure for Synthesis of Compounds 32. Compound **82** (2.62 g, 10 mmol), **76** (1.1 equiv), CuI (0.2 equiv), and PdCl₂(PPh₃)₂ (0.1 equiv) in DMF and TEA solvent were placed in a 25 mL round-bottom flask under Ar. Then, the mixture was stirred for 4 h at 100 °C. After this time, H₂O was added into the resulting complex and extracted with EtOAc three times. The organic layer was again washed with H₂O before being dried over MgSO₄, and the solvent was removed under vacuum leaving the crude product. The pure product was obtained by flash column chromatography (hexane/EtOAc = 4:1). Then, **83** was obtained through deprotection by TFA in DCM in 90% yield.

K₂CO₃ (1.2 equiv) and KI (0.2 equiv) were added to a solution of the deprotected intermediate **83** (1.94 g, 8 mmol) *tert*-butyl 4-bromopiperidine-1-carboxylate (1.2 equiv) in CH₃CN. After stirring the mixture overnight at 100 °C, the solvents were evaporated under reduced pressure to afford the corresponding crude compound 4-((4-(methoxycarbonyl)phenyl)ethynyl)-[1,4'-bipiperidine]-1'-carboxy-

late, which was purified by flash column chromatography (DCM/MeOH = 20:1) in 85% yield. NaOH (2 equiv) was added to a solution of *tert*-butyl 4-((4-(methoxycarbonyl)phenyl)ethynyl)-[1,4'-bipiperidine]-1'-carboxylate in MeOH/H₂O and stirred at rt for 2 h. Then, MeOH was removed under reduced pressure, the pH was adjusted with 2 N HCl, and the mixture was extracted with EtOAc. The solvent was removed to afford the product **84**, which was used without further purification.

To a solution of **86** (2.43 g, 10 mmol) in dry DMF was added NaH (1.2 equiv) at 0 °C. After stirring the mixture at 0 °C for 20 min, **85** was added and the mixture was stirred at rt for 4 h. After UPLC–MS demonstrated the full conversion of starting materials, H₂O was added and the mixture was extracted with EtOAc, the combined organic layers were washed with brine, and then dried over anhydrous Na₂SO₄. The solvent was removed on a rotary evaporator. The desired intermediate **87** was obtained by deprotection with TFA in DCM in 88% yield.

DIPEA (5 equiv) and HATU (1.2 equiv) were added to a solution of compounds **87** (278 mg, 1 mmol) and **84** (1.1 equiv) in DMF (2 mL). After 30 min at rt, the mixture was subjected to HPLC purification to afford compound **88** in 88% yield after deprotection in TFA/DCM.

DIPEA (5 equiv) and HATU (1.2 equiv) were added to a solution of compounds **88** (57.2 mg, 0.1 mmol) and **63** (1.1 equiv) in DMF (2 mL). After 30 min at rt, the mixture was subject to HPLC purification to afford compound **89** in 80% yield after deprotection in TFA/DCM.

DIPEA (5 equiv) and HATU (1.2 equiv) were added to a solution of compounds **89** (40.8 mg, 0.05 mmol) and **68** (1.1 equiv) in DMF (2 mL). After 30 min at rt, the mixture was subject to HPLC purification to afford compound **32** in 83% yield.

(2*S*,4*R*)-*N*-((*S*)-3-(4-(((1*r*,3*r*)-3-(3-Chloro-4-cyanophenoxy)-2,2,4,4-tetramethyl-cyclobutyl)carbamoyl)phenyl)ethynyl)-[1,4'-bipiperidin]-1'-yl)-1-(4-(4-methylthiazol-5-yl)phenyl)-3-oxopropyl-4-hydroxy-1-((*R*)-3-methyl-2-(3-methylisoxazol-5-yl)butanoyl)pyrrolidine-2-carboxamide (**32**). ¹H NMR (400 MHz, MeOD-*d*₄) δ 9.16 (t, *J* = 5.8 Hz, 1H), 7.81 (t, *J* = 8.8 Hz, 2H), 7.74 (d, *J* = 8.7 Hz, 1H), 7.59 (d, *J* = 7.5 Hz, 1H), 7.52 (dd, *J* = 9.1, 5.7 Hz, 5H), 7.14 (d, *J* = 2.1 Hz, 1H), 7.00 (dd, *J* = 8.7, 2.1 Hz, 1H), 6.33–6.20 (m, 1H), 5.53–5.37 (m, 1H), 4.70 (t, *J* = 12.9 Hz, 1H), 4.46 (t, *J* = 18.4 Hz, 2H), 4.31 (s, 2H), 4.17 (s, 1H), 3.90 (dd, *J* = 10.8, 3.8 Hz, 1H), 3.85–3.75 (m, 1H), 3.67–3.51 (m, 4H), 3.28–3.08 (m, 4H), 3.01–2.88 (m, 1H), 2.67 (dd, *J* = 24.1, 11.9 Hz, 1H), 2.56–2.51 (m, 3H), 2.48–2.32 (m, 2H), 2.27 (d, *J* = 4.2 Hz, 3H), 2.25–2.06 (m, 6H), 1.98 (dd, *J* = 10.1, 5.0 Hz, 3H), 1.77 (dd, *J* = 29.2, 14.2 Hz, 1H), 1.62–1.42 (m, 1H), 1.30 (s, 6H), 1.25 (s, 6H), 1.07 (dd, *J* = 13.4, 6.7 Hz, 3H), 0.91–0.84 (m, 3H). UPLC–MS calcd for C₆₁H₇₂ClN₉O₇S [M + H]⁺: 1095.49, found 1095.55. UPLC-retention time: 5.4 min.

General Procedure for Synthesis of Compound 33. Compound **99** (1.0 equiv) in acetone was added slowly at 0 °C to a solution of the intermediate **100** (0.4 g, 4 mmol) and Na₂CO₃ (1.5 equiv) in acetone. Then, the mixture was refluxed overnight. After UPLC–MS demonstrated the full conversion of starting materials, the solvents were evaporated under reduced pressure to afford the corresponding crude compound **101** that was purified by flash column chromatography (hexane/EtOAc = 4:1) in 95% yield.

A solution of the intermediate **101** (1.02 g, 3.8 mmol) and NH₂NH₂ (1.1 equiv) in EtOH was refluxed for 2 h. After UPLC–MS demonstrated the full conversion of starting materials, the solvents were evaporated under reduced pressure to afford the corresponding crude compound **102** that was purified by flash column chromatography (DCM/MeOH = 20:1) in 91% yield.

Compound **85** and 2-chloro-4-fluorobenzonitrile (1.5 equiv) were added at 0 °C to a mixture of **102** (0.8 g, 3 mmol) and NaH (1.2 equiv) in DMF and stirred for 5 min. The mixture was then stirred at rt for 3 h. After UPLC–MS demonstrated the full conversion of starting materials, ice/H₂O and brine were added into the mixture and the organic layer was collected and dried with Na₂SO₄. The solvent was removed on a rotary evaporator giving the desired intermediate (**103**), which was purified by flash column chromatography (hexane/EtOAc = 2:1) in 86% yield.

Compounds **103**, 4-(4-(4-bromobenzyl)-3,5-dimethyl-1*H*-pyrazol-1-yl)-2-chlorobenzonitrile (399 mg, 1 mmol), **92**, *tert*-butyl 4-ethynyl-

[1,4'-bipiperidine]-1'-carboxylate (1.1 equiv), CuI (0.2 equiv), and PdCl₂(PPh₃)₂ (0.1 equiv) in DMF and TEA solvent were placed in a 25 mL round-bottom flask under Ar. Then, the mixture was stirred 4 h at 100 °C and H₂O was added into the resulting complex, which was extracted with EtOAc three times. The organic layer was again washed with H₂O before being dried over MgSO₄ and the solvent was removed under vacuum leaving the crude product. The pure product was obtained by flash column chromatography (DCM/MeOH = 20:1). Compound **104** was obtained through deprotection by TFA in DCM (80% yield).

DIPEA (5 equiv) and HATU (1.2 equiv) were added to a solution of compounds **104** (51.1 mg, 0.1 mmol) and **63** (1.1 equiv) in DMF (2 mL). After 30 min at rt, the mixture was subject to HPLC purification to afford compound **105** in 84% yield after deprotection in TFA/DCM.

DIPEA (5 equiv) and HATU (1.2 equiv) were added to a solution of compounds **105** (60 mg, 0.08 mmol) and **68** (1.1 equiv) in DMF (2 mL). After 30 min at rt, the mixture was subject to HPLC purification to afford compound **33** in 81% yield.

(2*S*,4*R*)-*N*-((*S*)-3-(4-(((1*r*,3*r*)-3-(3-Chloro-4-cyanophenyl)-3,5-dimethyl-1*H*-pyrazol-4-yl)methyl)phenyl)ethynyl)-[1,4'-bipiperidin]-1'-yl)-1-(4-(4-methylthiazol-5-yl)phenyl)-3-oxopropyl-4-hydroxy-1-((*R*)-3-methyl-2-(3-methylisoxazol-5-yl)butanoyl)pyrrolidine-2-carboxamide (**33**). ¹H NMR (400 MHz, MeOD-*d*₄) δ = 8.94 (s, 1H), 7.92 (d, *J* = 8.4 Hz, 2H), 7.84 (s, 1H), 7.64 (d, *J* = 8.4 Hz, 1H), 7.50–7.45 (m, 4H), 7.39–7.26 (m, 2H), 7.14 (dd, *J* = 8.8 Hz, *J* = 8.4 Hz, 2H), 6.22 (s, 1H), 4.46 (s, 1H), 3.85–3.76 (m, 6H), 2.56–2.44 (m, 6H), 2.25 (s, 3H), 2.13 (s, 3H), 1.10–0.95 (m, 6H), 0.94–0.78 (m, 6H). UPLC–MS calcd for C₅₈H₆₅ClN₉O₅S [M + H]⁺: 1034.45, found 1034.65. UPLC-retention time: 5.1 min.

General Procedure for Synthesis of Compounds 34–38. Following the procedures used to prepare compound **32**, compounds **34–38** were obtained using the same methods.

(2*S*,4*R*)-*N*-((*S*)-3-(4-(((1*r*,3*r*)-3-(3-Chloro-4-cyanophenoxy)-2,2,4,4-tetramethyl-cyclobutyl)carbamoyl)phenyl)ethynyl)-[1,4'-bipiperidin]-1'-yl)-1-(4-(4-methylthiazol-5-yl)phenyl)-3-oxopropyl-1-((*S*)-2-(1-fluorocyclopropane-1-carboxamido)-3,3-dimethylbutanoyl)-4-hydroxypyrrolidine-2-carboxamide (**34**). ¹H NMR (400 MHz, MeOD-*d*₄) δ 9.19 (s, 1H), 7.81 (dd, *J* = 10.6, 7.6 Hz, 2H), 7.76–7.71 (m, 1H), 7.54 (t, *J* = 12.6 Hz, 6H), 7.15 (d, *J* = 5.2 Hz, 1H), 7.00 (t, *J* = 6.6 Hz, 1H), 5.42 (s, 1H), 4.68 (dd, *J* = 38.4, 26.4 Hz, 3H), 4.48 (s, 1H), 4.31 (d, *J* = 4.9 Hz, 1H), 4.20 (t, *J* = 12.0 Hz, 2H), 3.98–3.75 (m, 2H), 3.51 (s, 4H), 3.23–2.84 (m, 5H), 2.65 (d, *J* = 13.2 Hz, 1H), 2.60–2.52 (m, 3H), 2.20 (dt, *J* = 90.9, 52.2 Hz, 9H), 1.73–1.36 (m, 4H), 1.31 (d, *J* = 5.0 Hz, 6H), 1.25 (d, *J* = 5.7 Hz, 6H), 1.08 (d, *J* = 5.8 Hz, 9H). ¹³C NMR (100 MHz, MeOD-*d*₄) δ 171.80, 170.39, 170.12, 169.93, 169.04, 162.97, 152.32, 141.82, 137.56, 135.37, 134.11, 133.98, 131.45, 131.26, 129.99, 129.09, 127.35, 126.30, 126.07, 116.61, 116.06, 115.78, 114.31, 113.24, 104.36, 92.08, 90.65, 84.38, 80.80, 79.03, 76.73, 69.56, 63.45, 59.57, 59.51, 59.06, 57.37, 56.75, 50.63, 50.43, 46.07, 44.04, 43.93, 40.34, 39.94, 38.11, 37.95, 37.44, 36.40, 35.86, 29.44, 27.74, 26.49, 26.08, 25.57, 23.99, 23.07, 22.31, 14.09, 12.75, 12.61, 12.51. UPLC–MS calcd for C₆₂H₇₅ClF₈O₇S [M + H]⁺: 1129.52, found 1129.46. UPLC-retention time: 4.8 min.

(2*S*,4*R*)-*N*-((*S*)-3-(4-(((1*r*,3*r*)-3-(3-Chloro-4-cyanophenoxy)-2,2,4,4-tetramethyl-cyclobutyl)carbamoyl)phenyl)ethynyl)-[1,4'-bipiperidin]-1'-yl)-1-(4-(4-methylthiazol-5-yl)phenyl)-3-oxopropyl-1-((*S*)-2-(1-cyanocyclopropane-1-carboxamido)-3,3-dimethylbutanoyl)-4-hydroxypyrrolidine-2-carboxamide (**35**). ¹H NMR (400 MHz, MeOD-*d*₄) δ 9.77 (s, 1H), 7.85–7.77 (m, 2H), 7.74 (d, *J* = 8.6 Hz, 1H), 7.64–7.48 (m, 6H), 7.15 (s, 1H), 7.00 (d, *J* = 8.6 Hz, 1H), 5.46 (d, *J* = 5.4 Hz, 1H), 4.68 (d, *J* = 6.0 Hz, 2H), 4.58 (d, *J* = 7.4 Hz, 1H), 4.47 (s, 1H), 4.31 (s, 1H), 4.18 (s, 1H), 3.79 (d, *J* = 12.6 Hz, 2H), 3.58 (d, *J* = 9.4 Hz, 3H), 3.41 (s, 1H), 3.14 (d, *J* = 20.9 Hz, 3H), 2.94 (d, *J* = 6.5 Hz, 1H), 2.88–2.69 (m, 1H), 2.61 (d, *J* = 4.1 Hz, 3H), 2.46–2.04 (m, 7H), 1.99 (d, *J* = 7.0 Hz, 2H), 1.74–1.51 (m, 6H), 1.31 (s, 6H), 1.25 (s, 6H), 1.13–1.03 (m, 9H). UPLC–MS calcd for C₆₃H₇₄ClN₉O₅S [M + H]⁺: 1136.52, found 1136.56. UPLC-retention time: 4.6 min.

(2*S*,4*R*)-1-((*S*)-2-Acetamido-3,3-dimethylbutanoyl)-*N*-((*S*)-3-(4-(((1*r*,3*r*)-3-(3-chloro-4-cyanophenoxy)-2,2,4,4-tetramethylcyclobutyl)carbamoyl)phenyl)ethynyl)-[1,4'-bipiperi-

din]-1'-yl)-1-(4-(4-methylthiazol-5-yl)phenyl)-3-oxopropyl)-4-hydroxypyrrolidine-2-carboxamide (**36**). ¹H NMR (400 MHz, MeOD-*d*₄) δ 8.96 (s, 1H), 7.88–7.73 (m, 4H), 7.59 (d, *J* = 8.0 Hz, 1H), 7.51 (d, *J* = 6.7 Hz, 6H), 7.15 (d, *J* = 2.6 Hz, 1H), 7.00 (dd, *J* = 8.8, 2.6 Hz, 1H), 5.37 (s, 2H), 4.75–4.44 (m, 9H), 4.31 (s, 1H), 4.25–4.11 (m, 2H), 3.85 (dd, *J* = 48.9, 10.8 Hz, 2H), 3.53 (s, 3H), 3.09 (s, 6H), 2.90 (d, *J* = 13.8 Hz, 1H), 2.64 (d, *J* = 14.0 Hz, 1H), 2.55–2.47 (m, 3H), 2.16 (s, 6H), 2.01 (dd, *J* = 7.3, 3.4 Hz, 3H), 1.61 (s, 1H), 1.31 (s, 6H), 1.25 (s, 6H), 1.05 (d, *J* = 5.2 Hz, 9H). UPLC–MS calcd for C₆₀H₇₄ClN₈O₇S [M + H]⁺: 1085.51, found 1085.62. UPLC-retention time: 5.1 min.

(2*S*,4*R*)-*N*-((*R*)-3-(4-(((1*r*,3*r*)-3-(3-Chloro-4-cyanophenoxy)-2,2,4,4-tetramethyl-cyclobutyl)carbamoyl)phenyl)ethynyl)-[1,4'-bipiperidin]-1'-yl)-1-(4-(4-methylthiazol-5-yl)phenyl)-3-oxopropyl)-1-((*S*)-2-(1-fluorocyclopropane-1-carboxamido)-3,3-dimethyl-butano-yl)-4-hydroxypyrrolidine-2-carboxamide (**37**). ¹H NMR (400 MHz, MeOD-*d*₄) δ 9.56 (s, 1H), 7.81 (dd, *J* = 10.1, 8.1 Hz, 2H), 7.74 (d, *J* = 8.8 Hz, 1H), 7.72–7.64 (m, 2H), 7.60 (d, *J* = 8.1 Hz, 1H), 7.53 (dt, *J* = 16.5, 5.9 Hz, 3H), 7.15 (d, *J* = 2.4 Hz, 1H), 7.00 (dd, *J* = 8.8, 2.5 Hz, 1H), 5.46–5.40 (m, 1H), 4.77–4.49 (m, 4H), 4.31 (d, *J* = 2.4 Hz, 1H), 4.18 (d, *J* = 2.9 Hz, 2H), 3.88–3.74 (m, 2H), 3.57 (s, 4H), 3.21–2.88 (m, 5H), 2.74–2.65 (m, 1H), 2.58 (d, *J* = 5.2 Hz, 3H), 2.41–1.96 (m, 9H), 1.86–1.39 (m, 4H), 1.31 (d, *J* = 2.6 Hz, 6H), 1.25 (s, 6H), 1.06–0.96 (m, 9H). UPLC–MS calcd for C₆₂H₇₄ClFN₈O₇S [M + H]⁺: 1129.52, found 1129.58. UPLC-retention time: 4.9 min.

(2*S*,4*R*)-*N*-((*S*)-3-(4-(((1*r*,3*r*)-3-(3-Chloro-4-cyanophenoxy)-2,2,4,4-tetramethyl-cyclobutyl)carbamoyl)phenyl)ethynyl)-[1,4'-bipiperidin]-1'-yl)-1-(4-(4-methylthiazol-5-yl)phenyl)-3-oxopropyl)-1-((*R*)-2-(1-fluorocyclopropane-1-carboxamido)-3,3-dimethyl-butano-yl)-4-hydroxypyrrolidine-2-carboxamide (**38**). ¹H NMR (400 MHz, MeOD-*d*₄) δ 9.55 (s, 1H), 7.81 (dd, *J* = 12.3, 8.3 Hz, 2H), 7.73 (d, *J* = 8.7 Hz, 1H), 7.63–7.49 (m, 6H), 7.13 (d, *J* = 2.4 Hz, 1H), 6.99 (dt, *J* = 8.9, 1.7 Hz, 1H), 5.44 (d, *J* = 6.6 Hz, 1H), 4.72 (s, 1H), 4.59 (dt, *J* = 17.8, 4.7 Hz, 2H), 4.49 (s, 1H), 4.30 (d, *J* = 2.2 Hz, 1H), 4.17 (d, *J* = 2.7 Hz, 2H), 3.95 (dd, *J* = 10.1, 4.0 Hz, 1H), 3.75 (dt, *J* = 12.5, 4.3 Hz, 1H), 3.56 (s, 3H), 3.40 (s, 1H), 3.22–2.95 (m, 5H), 2.74–2.64 (m, 1H), 2.58 (d, *J* = 5.6 Hz, 3H), 2.36–1.98 (m, 9H), 1.87–1.45 (m, 3H), 1.41–1.34 (m, 2H), 1.30 (d, *J* = 2.5 Hz, 6H), 1.24 (s, 6H), 1.17–1.10 (m, 9H). UPLC–MS calcd for C₆₂H₇₄ClFN₈O₇S [M + H]⁺: 1129.52, found 1129.56. UPLC-retention time: 4.8 min.

General Procedure for Synthesis of Compound 39. DIPEA (5 equiv) and HATU (1.2 equiv) were added to a solution of compounds **87** (27.8 mg, 0.1 mmol) and **106** (1.1 equiv) in DMF (2 mL). After 30 min at rt, the mixture was subject to HPLC purification to afford compound **107** in 80% yield.

NaOH (2 equiv) was added to a solution of **107** (35 mg, 0.08 mmol) in MeOH/H₂O and stirred at rt for 2 h. Then, MeOH was removed under reduced pressure, the pH was adjusted to acidity with 2 M HCl, and the mixture was extracted with EtOAc. The solvent was removed to afford the product **108**, which was used without further purification.

DIPEA (5 equiv) and HATU (1.2 equiv) were added to a solution of compound **108** (33 mg, 0.08 mmol) and *tert*-butyl (9-aminononyl)-carbamate (1.1 equiv) in DMF (2 mL). After 30 min at rt, the mixture was subject to HPLC purification to afford compound **109** in 85% yield.

DIPEA (5 equiv) and HATU (1.2 equiv) were added to a solution of compounds **109** (39 mg, 0.07 mmol) and **63** (1.1 equiv) in DMF (2 mL). After 30 min at rt, the mixture was subject to HPLC purification to afford compound **110** in 84% yield after deprotection in TFA/DCM.

DIPEA (5 equiv) and HATU (1.2 equiv) were added to a solution of compounds **110** (40.5 mg, 0.05 mmol) and **68** (1.1 equiv) in DMF (2 mL). After 30 min at rt, the mixture was subject to HPLC purification to afford compound **39** in 84% yield.

N-(((1*r*,3*r*)-3-(3-Chloro-4-cyanophenoxy)-2,2,4,4-tetramethyl-cyclobutyl)-*N*-(9-((*S*)-3-((2*S*,4*R*)-4-hydroxy-1-((*R*)-3-methyl-2-(3-methylisoxazol-5-yl)butanoyl)pyrrolidine-2-carboxamido)-3-(4-(4-methylthiazol-5-yl)phenyl)propanamido)nonyl)terephthalamide (**39**). ¹H NMR (400 MHz, MeOD-*d*₄) δ 8.95 (s, 1H), 7.99–7.89 (m, 4H), 7.74 (dd, *J* = 8.8, 1.4 Hz, 1H), 7.48 (t, *J* = 4.8 Hz, 4H), 7.15 (t, *J* = 1.9 Hz, 1H), 7.00 (dt, *J* = 8.7, 1.8 Hz, 1H), 6.29–6.18 (m, 1H), 5.41–5.31 (m, 1H), 4.99 (s, 2H), 4.50 (dd, *J* = 17.3, 9.2 Hz, 2H), 4.31 (s, 1H), 4.20 (s, 1H), 3.89 (dd, *J* = 10.7, 4.3 Hz, 1H), 3.83–3.75 (m, 1H), 3.61 (d, *J* = 10.4 Hz, 1H), 3.38 (dd, *J* = 14.0, 7.1 Hz, 7H), 3.16–3.03 (m,

2H), 2.91–2.73 (m, 2H), 2.51 (d, *J* = 1.4 Hz, 3H), 2.42 (dq, *J* = 13.2, 6.8 Hz, 1H), 2.32–2.24 (m, 3H), 2.17 (t, *J* = 10.5 Hz, 1H), 2.00 (dq, *J* = 17.5, 6.5, 5.2 Hz, 1H), 1.68–1.56 (m, 2H), 1.35–1.24 (m, 18H), 1.16 (s, 1H), 1.11–1.04 (m, 3H), 0.93–0.84 (m, 3H). UPLC–MS calcd for C₅₉H₇₄ClN₈O₈S [M + H]⁺: 1089.50, found 1089.57. UPLC-retention time: 6.1 min.

General Procedure for Synthesis of Compound 40. DIPEA (5 equiv) and HATU (1.2 equiv) were added to a solution of compound **108** (42.6 mg, 0.1 mmol) and *tert*-butyl-(10-aminodecyl)carbamate (1.1 equiv) in DMF (2 mL). After 30 min at rt, the mixture was subject to HPLC purification to afford compound **112** in 80% yield.

DIPEA (5 equiv) was added to a solution of compound **112** (46.4 mg, 0.08 mmol) and 2-(2,6-dioxopiperidin-3-yl)-4-fluoroisindoline-1,3-dione (1.1 equiv) in DMSO (2 mL). After 4 h at 80 °C, the mixture was subject to HPLC purification to afford compound **40** in 90% yield.

N-(((1*r*,3*r*)-3-(3-Chloro-4-cyanophenoxy)-2,2,4,4-tetramethyl-cyclobutyl)-*N*-(10-((2-(2,6-dioxopiperidin-3-yl)-1,3-dioxoisindolin-4-yl)amino)decyl)terephthalamide (**40**). ¹H NMR (400 MHz, DMSO-*d*₆) δ 11.10 (s, 1H), 8.56 (t, *J* = 5.6 Hz, 1H), 8.01–7.87 (m, 7H), 7.64–7.56 (m, 1H), 7.21 (d, *J* = 2.4 Hz, 1H), 7.08 (d, *J* = 8.6 Hz, 1H), 7.04–6.95 (m, 2H), 6.52 (t, *J* = 5.9 Hz, 1H), 5.06 (dd, *J* = 12.9, 5.4 Hz, 1H), 4.34 (s, 1H), 4.13–4.08 (m, 1H), 3.30–3.24 (m, 4H), 2.94–2.84 (m, 1H), 2.68–2.51 (m, 3H), 2.05 (ddd, *J* = 12.7, 6.9, 2.9 Hz, 1H), 1.56 (dq, *J* = 14.2, 6.7 Hz, 5H), 1.33–1.28 (m, 10H), 1.25 (s, 6H), 1.15 (s, 6H). UPLC–MS calcd for C₄₆H₅₄ClN₆O₇ [M + H]⁺: 837.37, found 837.46. UPLC-retention time: 6.8 min.

General Procedure for Synthesis of Compound 41. DIPEA (5 equiv) was added to a solution of compound **88** (57.2 mg, 0.1 mmol) and 2-(2,6-dioxopiperidin-3-yl)-4-fluoroisindoline-1,3-dione (1.1 equiv) in DMSO (2 mL). After 4 h at 80 °C, the mixture was subject to HPLC purification to afford compound **41** in 88% yield.

N-(((1*r*,3*r*)-3-(3-Chloro-4-cyanophenoxy)-2,2,4,4-tetramethyl-cyclobutyl)-4-((1'-(2-(2,6-dioxopiperidin-3-yl)-1,3-dioxoisindolin-4-yl)-[1,4'-bipiperidin]-4-yl)ethynyl)benzamide (**41**). ¹H NMR (400 MHz, DMSO-*d*₆) δ = 11.1 (br, NH(CO)₂, 1H), 9.37 (s, CONH, 1H), 7.9 (d, 1H), 7.8 (d, 1H), 7.7 (d, 1H), 7.5 (dd, 1H), 7.4 (t, 1H), 7.2 (s, 1H), 7.0 (d, 1H), 6.5 (m, 3H), 5.7 (s, 4H), 5.1 (m, 1H), 4.1 (m, 3H), 3.8 (s, 1H), 3.5 (m, 2H), 3.2 (m, 3H), 3.0 (m, 3H), 2.6 (m, 1H), 2.2 (m, 3H), 2.1 (m, 2H), 1.9 (m, 2H), 1.2 (m, 12H). UPLC–MS calcd for C₄₇H₅₀ClN₆O₆ [M + H]⁺: 829.35, found 829.38. UPLC-retention time: 5.5 min.

Cell Lines and Cell Culture. All of the LNCaP, VCaP, and 22Rv1 cells used were purchased from American Type Culture Collection (ATCC). LNCaP and 22Rv1 cells were grown in RPMI 1640 (Invitrogen), and VCaP cells were grown in Dulbecco's modified Eagle's medium with Glutamax (Invitrogen). All of the cells were supplemented with 10% fetal bovine serum (Invitrogen) at 37 °C in a humidified 5% CO₂ incubator.

Quantitative Real-Time Polymerase Chain Reaction (qRT-PCR). Real-time PCR was performed using QuantStudio 7 Flex Real-Time PCR System as described previously.^{43,44} RNA was purified using the Qiagen RNase-Free DNase set, then after quantification, the extracted RNA was converted to cDNA using High Capacity RNA-to-cDNA Kit from Applied Biosystems (Thermo Fisher Scientific). The levels of AR, TMPRSS2, FKBPS, PSA(KLK3), and GAPDH were quantified using TaqMan Fast Advanced Master Mix from Applied Biosystems (see Table 6 for primer information). The level of gene expression was evaluated using comparative CT method, which compares the CT value to GAPDH (ΔCT) and then to vehicle control (ΔΔCT).

Cloning and Purification of VHL–ElonginBC Complex. The DNA sequence of VHL (coding for residues 54–213) was constructed by PCR and inserted into a His-TEV expression vector⁴⁵ using ligation-independent cloning. The DNA sequences of Elongin B (encoding residues 1–118) and Elongin C (encoding residues 1–96) were constructed by PCR and inserted into pCDFDuet 1 using Gibson assembly.⁴⁶ BL21(DE3) cells were transformed simultaneously with both plasmids and grown in terrific broth at 37 °C until an OD₆₀₀ of 1.2. The cells were induced overnight with 0.4 mM isopropyl β-D-1-thiogalactopyranoside at 24 °C. Pelleted cells were freeze–thawed and

Table 6. Antibodies and Reagents^a

reagent or resource	source	identifier
Antibodies		
GAPDH(14C10)	CST	Cat# 3683S
AR	ABCAM	Cat# ab194196 EPR1535(2)
secondary antibody conjugated with HRP	Invitrogen	Cat# A16172
Chemicals		
enzalutamide	1Click Chemistry	Cat# 915087-33-1
MG132 proteasome inhibitor	Selleck Chemicals	Cat# S2619
Primers		
TMPRSS2 qPCR	Applied Biosystems	Cat# Hs01122322_m1
FKBP5 qPCR	Applied Biosystems	Cat# Hs01561006_m1
KLK3 qPCR	Applied Biosystems	Cat# Hs02576345_m1
AR qPCR	Applied Biosystems	Cat# Hs00171172_m1
GAPDH qPCR	Applied Biosystems	Cat# Hs99999905_m1
ERG qPCR	Applied Biosystems	Cat# Hs01554634_m1

^aCell viability was evaluated by a WST-8 assay (Dojindo) following the manufacturer's instructions. Western blot analysis was performed as previously described.^{41,42}

then resuspended in 20 mM Tris–HCl pH 7.0, 200 mM NaCl, and 0.1% β -mercaptoethanol (BME) containing protease inhibitors. The cell suspension was lysed by sonication, and debris was removed via centrifugation. The supernatant was incubated at 4 °C for 1 h with Ni-NTA (Qiagen) prewashed in 20 mM Tris–HCl pH 7.0, 200 mM NaCl, and 10 mM imidazole. The protein complex was eluted in 20 mM Tris–HCl pH 7.0, 200 mM NaCl, and 300 mM imidazole; dialyzed into 20 mM Tris–HCl pH 7.0, 150 mM NaCl, and 0.01% BME; and incubated with TEV protease overnight at 4 °C. The protein sample was reapplied to the Ni-NTA column to remove the His-tag. The flow through containing the VHL complex was diluted to 75 mM NaCl and applied to a HiTrap Q column (GE Healthcare). The sample was eluted with a salt gradient (0.075–1 M NaCl), concentrated, and further purified on a Superdex S75 column (GE Healthcare) pre-equilibrated with 20 mM Bis-Tris 7.0, 150 mM NaCl, and 1 mM dithiothreitol. The samples were aliquoted and stored at –80 °C.

Binding Affinities of VHL Ligands to VHL–ElonginBC Complex Protein. The IC₅₀ and K_i values of compounds were determined in competitive binding experiments. Mixtures of 5 μ L of solutions of compounds in DMSO and 95 μ L of preincubated protein/tracer complex solution were added into assay plates incubated at room temperature for 60 min with gentle shaking. The final concentrations of both VHL protein and fluorescent probe were 5 nM. Negative controls containing protein/probe complex only (equivalent to 0% inhibition) and positive controls containing only free probes (equivalent to 100% inhibition) were included in each assay plate. FP values in millipolarization (mP) units were measured using the Infinite M-1000 plate reader (Tecan U.S., Research Triangle Park, NC) in Microfluor 1 96-well, black, round-bottom plates (Thermo Fisher Scientific, Waltham, MA) at an excitation wavelength of 485 nm and an emission wavelength of 530 nm. IC₅₀ values were determined by nonlinear regression fitting of the competition curves. The K_i values of competitive inhibitors were obtained directly by nonlinear regression fitting, based on the K_D values of the probe and concentrations of the protein and probe in the competitive assays. All of the FP competitive experiments were performed in duplicate in three independent experiments.

Western Blotting. The treated cells were lysed by radio-immunoprecipitation assay buffer supplemented with protease and

phosphatase inhibitors. The cell lysates were separated by 4–12% sodium dodecyl sulfate-polyacrylamide gel electrophoresis gels and blotted into poly(vinylidene difluoride) membranes. Software ImageJ was used to quantify the percentage of AR degradation. The net protein bands and loading controls are calculated by deducting the background from the inverted band value. The final relative quantification values are the ratio of net band to net loading control.

Pharmacodynamics Studies in the VCaP Xenograft Models in Mice. All animal experiments were performed under the guidelines of the University of Michigan Committee for Use and Care of Animals and using an approved animal protocol (PI, Shaomeng Wang). Xenograft tumors were established by injecting 5 \times 10⁶ VCaP cells in 50% Matrigel subcutaneously on the dorsal side of severe combined immunodeficient (SCID) mice, obtained from Charles River, one tumor per mouse. When tumors reached \sim 100 mm³, the mice were randomly assigned to treatment and vehicle control groups. For pharmacodynamics analysis, resected control and treated VCaP xenograft tumor tissues were ground into powder in liquid nitrogen and lysed in CST lysis buffer with halt protease inhibitors. Tumor clarified lysates (20 μ g) were separated on 4–20% or 4–12% Novex gels. Western blots were performed as detailed in the previous section.

■ ASSOCIATED CONTENT

§ Supporting Information

The Supporting Information is available free of charge on the ACS Publications website at DOI: 10.1021/acs.jmedchem.8b01631.

Western blotting analysis of AR proteins in LNCaP, VCaP, and 22Rv1 cells treated with AR antagonists 4, 6 and all of the AR degraders; Western blotting analysis of AR antagonists 3–7 in LNCaP cells; ¹H NMR, ¹³C NMR, and UPLC–MS spectra of compound 34; chemical data for VHL-a–h; chemical and biological data for VHL tracer HXC78 and biotin HXC79 (PDF)

Molecular string files for all of the final target compounds (CSV)

■ AUTHOR INFORMATION

Corresponding Author

*E-mail: shaomeng@umich.edu. Phone: 1-734-615-0362.

ORCID

Shaomeng Wang: 0000-0002-8782-6950

Present Address

▲C.W.: National Pharmaceutical Teaching Laboratory Center, School of Pharmaceutical Sciences, Peking University, Beijing 100191, China

Author Contributions

▽X.H., C.W., C.Q., and W.X. contributed equally to this work.

Notes

The authors declare the following competing financial interest(s): The University of Michigan has filed a patent application on these AR degraders, which has been licensed by Oncopia Therapeutics LLC. S. Wang, X. Han, C. Wang, C. Qin, W. Xiang, T. Xu, and C. Yang are co-inventors on these patents. The University of Michigan has received a research contract from Oncopia. S.W. is a co-founder of Oncopia, owns shares in Oncopia and is a paid consultant to Oncopia.

■ ACKNOWLEDGMENTS

This study was supported in part by funding from Oncopia Therapeutics, LLC, and the University of Michigan Comprehensive Cancer Center Core Grant from the National Cancer Institute, NIH (Grant P30CA046592).

■ ABBREVIATIONS

AR, androgen receptor; mCRPC, metastatic castration-resistant prostate cancer; PROTAC, proteolysis targeting chimera; PCa, prostate cancer; ADT, androgen deprivation therapies; SNIPERs, specific and nongenetic IAP-dependent protein erasers; cIAP1, cellular inhibitor of apoptosis protein 1; PEG, poly(ethylene glycol); FP, fluorescence polarization; ATCC, American Type Culture Collection; qRT-PCR, quantitative real-time polymerase chain reaction; SCID mice, severe combined immunodeficient mice

■ REFERENCES

- (1) Hamdy, F. C.; Donovan, J. L.; Lane, J. A.; Mason, M.; Metcalfe, C.; Holding, P.; Davis, M.; Peters, T. J.; Turner, E. L.; Martin, R. M.; Oxley, J.; Robinson, M.; Staffurth, J.; Walsh, E.; Bollina, P.; Catto, J.; Doble, A.; Doherty, A.; Gillatt, D.; Kockelbergh, R.; Kynaston, H.; Paul, A.; Powell, P.; Prescott, S.; Rosario, D. J.; Rowe, E.; Neal, D. E. 10-year outcomes after monitoring, surgery, or radiotherapy for localized prostate cancer. *N. Engl. J. Med.* **2016**, *375*, 1415–1424.
- (2) Litwin, M. S.; Tan, H. J. The diagnosis and treatment of prostate cancer. *JAMA, J. Am. Med. Assoc.* **2017**, *317*, 2532–2542.
- (3) Karantanos, T.; Corn, P. G.; Thompson, T. C. Prostate cancer progression after androgen deprivation therapy: mechanisms of castrate resistance and novel therapeutic approaches. *Oncogene* **2013**, *32*, 5501–5511.
- (4) Harris, W. P.; Mostaghel, E. A.; Nelson, P. S.; Montgomery, B. Androgen deprivation therapy: progress in understanding mechanisms of resistance and optimizing androgen depletion. *Nat. Clin. Pract. Neurol.* **2009**, *6*, 76–85.
- (5) Narayanan, R.; Ponnusamy, S.; Miller, D. D. Destroying the androgen receptor (AR)-potential strategy to treat advanced prostate cancer. *Oncoscience* **2017**, *4*, 175–177.
- (6) Crowder, C. M.; Lassiter, C. S.; Gorelick, D. A. Nuclear androgen receptor regulates testes organization and oocyte maturation in zebrafish. *Endocrinology* **2018**, *159*, 980–993.
- (7) Sundén, H.; Holland, M. C.; Poutiainen, P. K.; Jääskeläinen, T.; Pulkkinen, J. T.; Palvimo, J. J.; Olsson, R. Synthesis and biological evaluation of second-generation tropanol-based androgen receptor modulators. *J. Med. Chem.* **2015**, *58*, 1569–1574.
- (8) Oksala, R.; Moilanen, A.; Riikonen, R.; Rummakko, P.; Karjalainen, A.; Passiniemi, M.; Wohlfahrt, G.; Taavitsainen, P.; Malmström, C.; Ramela, M.; Metsänkylä, H. M.; Huhtaniemi, R.; Kallio, P. J.; Mustonen, M. V. Discovery and development of ODM-204: a novel nonsteroidal compound for the treatment of castration-resistant prostate cancer by blocking the androgen receptor and inhibiting CYP17A1. *J. Steroid Biochem. Mol. Biol.* **2018**, DOI: 10.1016/j.jsbmb.2018.02.004.
- (9) Watson, P. A.; Arora, V. K.; Sawyers, C. L. Emerging mechanisms of resistance to androgen receptor inhibitors in prostate cancer. *Nat. Rev. Cancer* **2015**, *15*, 701–711.
- (10) Guo, C.; Linton, A.; Kephart, S.; Ornelas, M.; Pairish, M.; Gonzalez, J.; Greasley, S.; Nagata, A.; Burke, B. J.; Edwards, M.; Hosea, N.; Kang, P.; Hu, W.; Engebretsen, J.; Briere, D.; Shi, M.; Gukasyan, H.; Richardson, P.; Dack, K.; Underwood, T.; Johnson, P.; Morell, A.; Felstead, R.; Kuruma, H.; Matsimoto, H.; Zoubeidi, A.; Gleave, M.; Los, G.; Fanjul, A. N. Discovery of aryloxy tetramethylcyclobutanes as novel androgen receptor antagonists. *J. Med. Chem.* **2011**, *54*, 7693–7704.
- (11) Moilanen, A. M.; Riikonen, R.; Oksala, R.; Ravanti, L.; Aho, E.; Wohlfahrt, G.; Nykänen, P. S.; Törmäkangas, O. P.; Palvimo, J. J.; Kallio, P. J. Discovery of ODM-201, a new generation androgen receptor inhibitor targeting resistance mechanisms to androgen signaling-directed prostate cancer therapies. *Sci. Rep.* **2015**, *5*, No. 12007.
- (12) Guerrini, A.; Tesei, A.; Ferroni, C.; Paganelli, G.; Zamagni, A.; Carloni, S. D.; Donato, M.; Castoria, G.; Leonetti, C.; Porru, M. D.; Cesare, M.; Zaffaroni, N.; Beretta, G. L. D.; Rio, A.; Varchi, G. A new avenue toward androgen receptor pan-antagonists: C2 sterically hindered substitution of hydroxy-propanamides. *J. Med. Chem.* **2014**, *57*, 7263–7279.
- (13) Jung, M. E.; Ouk, S.; Yoo, D.; Sawyers, C. L.; Chen, C.; Tran, C.; Wongvipat, J. Structure-activity relationship for thiohydantoin androgen receptor antagonists for castration-resistant prostate cancer (CRPC). *J. Med. Chem.* **2010**, *53*, 2779–2796.
- (14) Yamamoto, S.; Tomita, N.; Suzuki, Y.; Suzuki, T.; Kaku, T.; Hara, T.; Yamaoka, M.; Kanzaki, N.; Hasuoka, A.; Baba, A.; Ito, M. Design, synthesis, and biological evaluation of 4-arylmethyl-1-phenylpyrazole and 4-aryloxy-1-phenylpyrazole derivatives as novel androgen receptor antagonists. *Bioorg. Med. Chem.* **2012**, *20*, 2338–2352.
- (15) Balbas, M. D.; Evans, M. J.; Hosfield, D. J.; Wongvipat, J.; Arora, V. K.; Watson, P. A.; Chen, Y.; Greene, G. L.; Shen, Y.; Sawyers, C. L. Overcoming mutation-based resistance to antiandrogens with rational drug design. *Elife* **2013**, *2*, No. e00499.
- (16) Lottrup, G.; Jørgensen, A.; Nielsen, J. E.; Jørgensen, N.; Duno, M.; Vinggaard, A. M.; Skakkebak, N. E.; Rajpert-De Meyts, E. Identification of a novel androgen receptor mutation in a family with multiple components compatible with the testicular dysgenesis syndrome. *J. Clin. Endocrinol. Metab.* **2013**, *98*, 2223–2229.
- (17) Zhu, S.; Zhao, D.; Yan, L.; Jiang, W.; Kim, J. S.; Gu, B.; Liu, Q.; Wang, R.; Xia, B.; Zhao, J. C.; Song, G.; Mi, W.; Wang, R. F.; Shi, X.; Lam, H. M.; Dong, X.; Yu, J.; Chen, K.; Cao, Q. BMI1 regulates androgen receptor in prostate cancer independently of the polycomb repressive complex 1. *Nat. Commun.* **2018**, *9*, No. 500.
- (18) Munuganti, R. S.; Hassona, M. D.; Leblanc, E.; Frewin, K.; Singh, K.; Ma, D.; Ban, F.; Hsing, M.; Adomat, H.; Lallous, N.; Andre, C.; Jonadass, J. P.; Zoubeidi, A.; Young, R. N.; Guns, E. T.; Rennie, P. S.; Cherkasov, A. Identification of a potent antiandrogen that targets the BF3 site of the androgen receptor and inhibits enzalutamide-resistant prostate cancer. *Chem. Biol.* **2014**, *21*, 1476–485.
- (19) Raina, K.; Lu, J.; Qian, Y.; Altieri, M.; Gordon, D.; Rossi, A. M.; Wang, J.; Chen, X.; Dong, H.; Siu, K.; Winkler, J. D.; Crew, A. P.; Crews, C. M.; Coleman, K. G. PROTAC-induced BET protein degradation as a therapy for castration-resistant prostate cancer. *Proc. Natl. Acad. Sci. U.S.A.* **2016**, *113*, 7124–7129.
- (20) Zhou, B.; Hu, J.; Xu, F.; Chen, Z.; Bai, L.; Fernandez-Salas, E.; Lin, M.; Liu, L.; Yang, C. Y.; Zhao, Y.; McEachern, D.; Przybranowski, S.; Wen, B.; Sun, D.; Wang, S. Discovery of a small-molecule degrader of bromodomain and extra-terminal (BET) proteins with picomolar cellular potencies and capable of achieving tumor regression. *J. Med. Chem.* **2018**, *61*, 462–481.
- (21) Gadd, M. S.; Testa, A.; Lucas, X.; Chan, K. H.; Chen, W.; Lamont, D. J.; Zengerle, M.; Ciulli, A. Structural basis of PROTAC cooperative recognition for selective protein degradation. *Nat. Chem. Biol.* **2017**, *13*, 514–521.
- (22) Toure, M.; Crews, C. M. Small-molecule PROTACS: new approaches to protein degradation. *Angew. Chem., Int. Ed.* **2016**, *55*, 1966–1973.
- (23) Qin, C.; Hu, Y.; Zhou, B.; Fernandez-Salas, E.; Yang, C. Y.; Liu, L.; McEachern, D.; Przybranowski, S.; Wang, M.; Stuckey, J.; Meagher, J.; Bai, L.; Chen, Z.; Lin, M.; Yang, J.; Ziazadeh, D. N.; Xu, F.; Hu, J.; Xiang, W.; Huang, L.; Li, S.; Wen, B.; Sun, D.; Wang, S. Discovery of QCA570 as an Exceptionally Potent and Efficacious Proteolysis Targeting Chimera (PROTAC) Degradable of the Bromodomain and Extra-Terminal (BET) Proteins Capable of Inducing Complete and Durable Tumor Regression. *J. Med. Chem.* **2018**, *61*, 6685–6704.
- (24) Hatcher, J. M.; Wang, E. S.; Johannessen, L.; Kwiatkowski, N.; Sim, T.; Gray, N. S. Development of highly potent and selective steroidal inhibitors and degraders of CDK8. *ACS Med. Chem. Lett.* **2018**, *9*, 540–545.
- (25) Gollavilli, P. N.; Pawar, A.; Wilder-Romans, K.; Natesan, R.; Engelke, C. G.; Dommeti, V. L.; Krishnamurthy, P. M.; Nallasivam, A.; Apel, I. J.; Xu, T.; Qin, Z. S.; Feng, F. Y.; Asangani, I. A. EWS/ETS-driven ewing sarcoma requires BET bromodomain proteins. *Cancer Res.* **2018**, *78*, 4760–4773.
- (26) Bondeson, D. P.; Crews, C. M. Targeted protein degradation by Small Molecules. *Annu. Rev. Pharmacol. Toxicol.* **2017**, *57*, 107–123.

- (27) Salami, J.; Alabi, S.; Willard, R. R.; Vitale, N. J.; Wang, J.; Dong, H.; Jin, M.; McDonnell, D. P.; Crew, A. P.; Neklesa, T. K.; Crews, C. M. Androgen receptor degradation by the proteolysis-targeting chimera ARCC-4 outperforms enzalutamide in cellular models of prostate cancer drug resistance. *Commun. Biol.* **2018**, *1*, No. 100.
- (28) Pal, S. K.; Patel, J.; He, M.; Foulk, B.; Kraft, K.; Smirnov, D. A.; Twardowski, P.; Kortylewski, M.; Bhargava, V.; Jones, J. O. Identification of mechanisms of resistance to treatment with abiraterone acetate or enzalutamide in patients with castration-resistant prostate cancer (CRPC). *Cancer* **2018**, *124*, 1216–1224.
- (29) Wang, C.; Peng, G.; Huang, H.; Liu, F.; Kong, D. P.; Dong, K. Q.; Dai, L. H.; Zhou, Z.; Wang, K. J.; Yang, J.; Cheng, Y. Q.; Gao, X.; Qu, M.; Wang, H. R.; Zhu, F.; Tian, Q. Q.; Liu, D.; Cao, L.; Cui, X. G.; Xu, C. L.; Xu, D. F.; Sun, Y. H. Blocking the feedback loop between neuroendocrine differentiation and macrophages improves the therapeutic effects of enzalutamide (MDV3100) on prostate cancer. *Clin Cancer Res.* **2018**, *24*, 708–723.
- (30) Gustafson, J. L.; Neklesa, T. K.; Cox, C. S.; Roth, A. G.; Buckley, D. L.; Tae, H. S.; Sundberg, T. B.; Stagg, D. B.; Hines, J.; McDonnell, D. P.; Norris, J. D.; Crews, C. M. Small-molecule-mediated degradation of the androgen receptor through hydrophobic tagging. *Angew. Chem., Int. Ed.* **2015**, *54*, 9659–9662.
- (31) Shibata, N.; Nagai, K.; Morita, Y.; Ujikawa, O.; Ohoka, N.; Hattori, T.; Koyama, R.; Sano, O.; Imaeda, Y.; Nara, H.; Cho, N.; Naito, M. Development of protein degradation inducers of androgen receptor by conjugation of androgen receptor ligands and inhibitor of apoptosis protein ligands. *J. Med. Chem.* **2018**, *61*, 543–575.
- (32) Crew, A. P.; Dong, H. Q.; Wang, J.; Ferraro, C.; Chen, X.; Qian, Y. M. Compounds and Methods for the Targeted Degradation of Androgen Receptor. US20,170,327,469A12017.
- (33) de Jésus-Tran, K. P.; Côté, P. L.; Cantin, L.; Blanchet, J.; Labrie, F.; Breton, R. Comparison of crystal structures of human androgen receptor ligand-binding domain complexed with various agonists reveals molecular determinants responsible for binding affinity. *Protein Sci.* **2006**, *15*, 987–999.
- (34) Galdeano, C.; Gadd, M. S.; Soares, P.; Scaffidi, S.; Van Molle, I.; Birced, I.; Hewitt, S.; Dias, D. M.; Ciulli, A. Structure-guided design and optimization of small molecules targeting the protein-protein interaction between the von Hippel-Lindau (VHL) E3 ubiquitin ligase and the hypoxia inducible factor (HIF) alpha subunit with in vitro nanomolar affinities. *J. Med. Chem.* **2014**, *57*, 8657–8663.
- (35) Soares, P.; Gadd, M. S.; Frost, J.; Galdeano, C.; Ellis, L.; Epemolu, O.; Rocha, S.; Read, K. D.; Ciulli, A. Group-based optimization of potent and cell-active inhibitors of the von Hippel-Lindau (VHL) E3 ubiquitin ligase: structure-activity relationships leading to the chemical probe (2S,4R)-1-((S)-2-(1-Cyanocyclopropyl)-3,3-dimethylbutanoyl)-4-hydroxy-N-(4-(4-methylthiazol-5-yl)benzyl)pyrrolidine-2-carboxamide (VH298). *J. Med. Chem.* **2018**, *61*, 599–618.
- (36) Buckley, D. L.; Van Molle, I.; Gareiss, P. C.; Tae, H. S.; Michel, J.; Noblin, D. J.; Jorgensen, W. L.; Ciulli, A.; Crews, C. M. Targeting the von Hippel-Lindau E3 ubiquitin ligase using small molecules to disrupt the VHL/HIF-1 α interaction. *J. Am. Chem. Soc.* **2012**, *134*, 4465–4468.
- (37) Berlin, M.; Zimmerman, K.; Snyder, L.; Crew, A. P.; Crews, C. M.; Chen, X.; Dong, H. Q.; Ferraro, C.; Jin, M. H.; Qian, Y. M.; Siu, K.; Wang, J. Compounds and Methods for the Enhanced Degradation of Targeted Proteins. WO2016149668A12016.
- (38) Ishoey, M.; Chorn, S.; Singh, N.; Jaeger, M. G.; Brand, M.; Paulk, J.; Bauer, S.; Erb, M. A.; Parapatics, K.; Müller, A. C.; Bennett, K. L.; Ecker, G. F.; Bradner, J. E.; Winter, G. E. Translation termination factor GSPT1 is a phenotypically relevant off-target of heterobifunctional phthalimide degraders. *ACS Chem. Biol.* **2018**, *13*, 553–560.
- (39) Powell, C. E.; Gao, Y.; Tan, L.; Donovan, K. A.; Nowak, R. P.; Loehr, A.; Bahcall, M.; Fischer, E. S.; Jänne, P. A.; George, R. E.; Gray, N. S. Chemically induced degradation of anaplastic lymphoma kinase (ALK). *J. Med. Chem.* **2018**, *61*, 4249–4255.
- (40) Frost, J.; Galdeano, C.; Soares, P.; Gadd, M. S.; Grzes, K. M.; Ellis, L.; Epemolu, O.; Shimamura, S.; Bantscheff, M.; Grandi, P.; Read, K. D.; Cantrell, D. A.; Rocha, S.; Ciulli, A. Potent and selective chemical probe of hypoxic signalling downstream of HIF-alpha hydroxylation via VHL inhibition. *Nat. Commun.* **2016**, *7*, No. 13312.
- (41) Liu, V. W. S.; Yau, W. L.; Tam, C. W.; Yao, K. M.; Shiu, S. Y. W. Melatonin inhibits androgen receptor splice variant-7 (AR-V7)-induced nuclear factor-kappa B (NF- κ B) activation and NF- κ B activator-induced AR-V7 expression in prostate cancer cells: potential implications for the use of melatonin in castration-resistant prostate cancer (CRPC) therapy. *Int. J. Mol. Sci.* **2017**, *18*, No. 1130.
- (42) Sun, H.; Nikolovska-Coleska, Z.; Lu, J.; Meagher, J. L.; Yang, C. Y.; Qiu, S.; Tomita, Y.; Ueda, Y.; Jiang, S.; Krajewski, K.; Roller, P. P.; Stuckey, J. A.; Wang, S. Design, synthesis, and characterization of a potent, nonpeptide, cell-permeable, bivalent Smac mimetic that concurrently targets both the BIR2 and BIR3 domains in XIAP. *J. Am. Chem. Soc.* **2007**, *129*, 15279–15294.
- (43) Lu, J.; Bai, L.; Sun, H.; Nikolovska-Coleska, Z.; McEachern, D.; Qiu, S.; Miller, R. S.; Yi, H.; Shangary, S.; Sun, Y.; Meagher, J. L.; Stuckey, J. A.; Wang, S. SM-164: a novel, bivalent Smac mimetic that induces apoptosis and tumor regression by concurrent removal of the blockade of cIAP-1/2 and XIAP. *Cancer Res.* **2008**, *68*, 9384–9393.
- (44) Bai, L.; Zhou, B.; Yang, C. Y.; Ji, J.; McEachern, D.; Przybranowski, S.; Jiang, H.; Hu, J.; Xu, F.; Zhao, Y.; Liu, L.; Fernandez-Salas, E.; Xu, J.; Dou, Y.; Wen, B.; Sun, D.; Meagher, J.; Stuckey, J.; Hayes, D. F.; Li, S.; Ellis, M. J.; Wang, S. Targeted degradation of BET proteins in triple-negative breast cancer. *Cancer Res.* **2017**, *77*, 2476–2487.
- (45) Stols, L.; Gu, M.; Dieckman, L.; Raffin, R.; Collart, F. R.; Donnelly, M. I. A new vector for high-throughput, ligation-independent cloning encoding a tobacco etch virus protease cleavage site. *Protein Expression Purif.* **2002**, *25*, 8–15.
- (46) Benoit, R. M.; Ostermeier, C.; Geiser, M.; Li, J. S.; Widmer, H.; Auer, M. Seamless insert-plasmid assembly at high efficiency and low cost. *PLoS One* **2016**, *11*, No. e01513158.